The natural antisense transcript HAS2-AS1 regulates breast cancer cells aggressiveness independently from hyaluronan metabolism

Arianna Parnigoni [a,1], Ilaria Caon [a,1], Wei Xuan Teo [b,1], San Hue Hua [b], Paola Moretto [a], Barbara Bartolini [a], Manuela Viola [a], Evgenia Karousou [a], George W. Yip [b], Martin Götte [c], Paraskevi Heldin [d], Alberto Passi [a] and Davide Vigetti [a]

***a* - Department of Medicine and Surgery,** *University of Insubria, via J.H. Dunant 5, Varese 21100, Italy*
***b* - Department of Anatomy,** *Yong Loo Lin School of Medicine, National University of Singapore 4 Medical Drive, Block MD10, Singapore 117594, Singapore*
***c* - Department of Gynecology and Obstetrics,** *University Hospital Münster, Albert-Schweitzer-Campus 1, D11, Münster 48149, Germany*
***d* - Department Medical Biochemistry and Microbiology,** *Uppsala University, Uppsala, Sweden*

Corresponding to Davide Vigetti: *Department of Medicine and Surgery, University of Insubria, via J.H. Dunant 5, Varese 21100, Italy. Davide.vigetti@uninsubria.it.*
https://doi.org/10.1016/j.matbio.2022.03.009

Abstract

Hyaluronan (HA) is a ubiquitous extracellular matrix component playing a crucial role in the regulation of cell behaviors, including cancer. Aggressive breast cancer cells tend to proliferate, migrate and metastatize. Notably, triple-negative breast cancer cells lacking the expression of estrogen receptor (ER) as well as progesterone receptor and HER2 are more aggressive than ER-positive ones. As currently no targeted therapy is available for triple-negative breast cancer, the identification of novel therapeutic targets has a high clinical priority. In ER-negative cells, tumoral behavior can be reduced by inhibiting HA synthesis or silencing the enzymes involved in its metabolism, such as HA synthase 2 (HAS2). HAS2-AS1 is a long non-coding RNA belonging to the natural antisense transcript family which is known to favor HAS2 gene expression and HA synthesis, thus bolstering malignant progression in brain, ovary, and lung tumors. As the role of HAS2-AS1 has not yet been investigated in breast cancer, in this work we report that ER-positive breast cancers had lower HAS2-AS1 expression compared to ER-negative tumors. Moreover, the survival of patients with ER-negative tumors was higher when the expression of HAS2-AS1 was elevated. Experiments with ER-negative cell lines as MDA-MB-231 and Hs 578T revealed that the overexpression of either the full-length HAS2-AS1 or its exon 2 long or short isoforms alone, strongly reduced cell viability, migration, and invasion, whereas HAS2-AS1 silencing increased cell aggressiveness. Unexpectedly, in these ER-negative cell lines, HAS2-AS1 is involved neither in the regulation of HAS2 nor in HA deposition. Finally, transcriptome analysis revealed that HAS2-AS1 modulation affected several pathways, including apoptosis, proliferation, motility, adhesion, epithelial to mesenchymal transition, and signaling, describing this long non-coding RNA as an important regulator of breast cancer cells aggressiveness.

Introduction

Breast cancer is the most diagnosed cancer in women with over 2.3 million new cases in 2020 [1]. Based on the expression of specific markers (i.e., PAM50), breast cancer can be classified into four subtypes in which the growth of transformed cells can be driven by the activation of receptors as human epidermal growth factor receptor 2 (HER2), estrogen receptor (ER) and progesterone receptor

(PR) as well as the presence of *BRCA* mutations. The therapeutic strategies change in function of the cancer subtypes. As ER-expressing breast cancers can be specifically treated using estrogen antagonists (i.e., tamoxifen) in combination with aromatase inhibitors, they show a good prognosis and survival rate [2], whereas triple-negative breast cancers (TNBC, lacking the expression of HER2, ER, and PR), having no specific targets to point drugs, prognosis is poor [3].

Metastases are the most critical aspect of breast cancers representing the first cause of death for patients [4]. TNBC cells are highly aggressive with an elevated capability to disseminate to distant organs. The acquisition of an invasive phenotype is far to be fully understood. Critical factors supporting cancer cells spreading are the secretion of a complex cocktail of degradative enzymes aimed to disassemble the extracellular matrix (ECM) surroundings the tumor cells, as well as the synthesis of particular ECM components able to modulate cellular pathways, thus enhancing the hallmarks of cancer, such as proliferative signaling, evading growth suppressors, resisting cell death, enabling replicative immortality, inducing angiogenesis, activating invasion and metastasis, inducing abnormal metabolic pathways and evading the immune system [5,6].

ECM is so noteworthy not only because it determines the mechanical properties of tissues but also because cells can recognize ECM components, for example via integrins or other receptors, triggering a plethora of cellular responses [7]. ECM is composed of a mesh of structural proteins and glycosaminoglycans, which are attached to core proteins to form proteoglycans [8]. Hyaluronan (HA) is an unusual glycosaminoglycan as it is unsulphated and free from core proteins. It is composed of a huge number (i.e., 2000−25,000) of repeating disaccharide units of N-acetyl-glucosamine (GlcNAc) and glucuronic acid (GlcUA), with molecular mass ranging from 10^5 to 10^7 Da [9]. HA modulates cell motility, proliferation, differentiation, and inflammation by interacting with several membrane receptors like CD44 and receptor for HA-mediated motility (RHAMM) triggering protein tyrosine kinases, focal adhesion kinase and extracellular signal-regulated kinases (ERK) activation [10].

HA is one of the major matrix molecules accumulating in human breast malignancies [11,12], and the amount of HA in the tumor stroma or the neoplastic cell compartment impacts the overall outcome [13]. HA is associated with invasion, lymphangiogenesis, angiogenesis, epithelial to mesenchymal transition (EMT), metastases, and multidrug resistance [14,15]. Interestingly, as many tumors express high levels of CD44, HA can be also employed in functionalizing drug carriers (i.e., liposomes and nanoparticles) to target the treatment of neoplastic cells [16].

In mammals, HA metabolism depends on the activity of three different synthetic enzymes called HA synthases (HAS1, 2 and 3) located on the plasma membrane, as well as on different degrading enzymes called hyaluronidases [17]. Little is known about the specific role of HAS isoenzymes in pathophysiology. Among all HASes, the most important in humans is HAS2, which is widely expressed and finely regulated from transcriptional to post-translational level [18]. In ER-positive cancer cells as MCF-7, the expression of HASes and HA production is low [19]; interestingly, it was described that enhanced HA degradation, as well as HAS2 overexpression, decrease the expression of estrogen receptor favoring tumor growth [20,21]. Contrary to ER-positive tumor cells, in TNBC cell lines such as MDA-MB-231, HAS2 is dramatically upregulated leading to an abnormal HA accumulation and favoring tumors spreading [19,22−24]. The rapid HA turnover in TNBC leads to the production of low molecular mass HA that sustains invasive phenotypes [25,26]. The synthesis of HA in tumor cells is also supported by other pathways as the metabolic reprogramming of cancer cells that leads to an increase of anabolic precursors availability [27], altered O-GlcNAcylation which stabilizes HAS2 [28,29], vitamin D availability and vitamin D receptor expression [30] and pharmacological treatments [31]. Additionally, recent findings suggest that breast cancer cells secrete the new protein C10orf118 that induces stromal cells, like fibroblasts, to produce HA [32].

The crucial role of HA and HAS2 in breast cancers is demonstrated by the inhibition of HASes by using 4-methylumbelliferone (4-MU) and knocking down HAS2 which reduced both the spreading and growth of cancer cells [23,33−35]. However, 4-MU is not specific and inhibits all the HASes; moreover, by reducing the availability of UDP-GlcUA to form 4-MU glucuronide [36], 4-MU could affect other biochemical reactions as glucuronidations [14]. Further, 4-MU could cause potential detrimental effects as described for glycocalyx alteration in an animal model for atherosclerosis [37]. Therefore, other specific pathways involving HAS2 and regulating HA production should be identified, to find a potential target for new pharmacological treatments.

HAS2 possesses a complex and specific epigenetic regulation [38] that involves the long non-coding RNA (lncRNA) HAS2-AS1. lncRNAs are functional RNA molecules that are transcribed from DNA but not translated into proteins, although recently it has been described that some micropeptides can be translated from lnRNAs' short open reading frame [39,40], being able to regulate gene expression [41]. Specifically, the natural antisense transcript HAS2-AS1 is located on the opposite DNA strand of the *HAS2* gene on human chromosome 8, and we demonstrated that HAS2-AS1

regulates the chromatin structure around the *HAS2* promoter in human aortic smooth muscle cells by interacting with p65 and allowing an efficient HAS2 messenger transcription [42]. lncRNAs can also interact with proteins, mRNA, or microRNA (miRNA) in the cytosol and, indeed, HAS2-AS1 has been described to form a duplex with HAS2 transcript in renal cells favoring its stability [43]. Interestingly, HAS2-AS1 has two main isoforms due to alternative splicing on exon 2, generating exon 2 long (L) and short (S) isoforms of 174 and 257 bp, respectively [44], both sharing complementarity with exon 1 of HAS2 mRNA. The physiological role of these two isoforms is completely unknown.

The role HAS2-AS1 has been described in several malignancies where it generally increases aggressiveness. In fact, HAS2-AS1 favors invasiveness of oral squamous cell carcinoma [45], promotes tumor progression in glioblastoma [46–48], and induces epithelial ovarian cancer proliferation and invasion [49]. Further, HAS2-AS1 has been also described to accelerate non-small cell lung cancer chemotherapy resistance [50]. Surprisingly, the role of HAS2-AS1 in breast cancers is not yet deeply investigated although it is involved in mouse mammary gland epithelial cells transformation by Transforming growth factor-beta [51]. Therefore, this work aims to investigate the role of HAS2-AS1 in human cellular models of ER-positive and negative breast cancers.

Results

HAS2-AS1 expression is higher in TNBC and breast cancer tissues and is correlated with better overall survival

Although the expression of HAS2-AS1 was already demonstrated in aggressive breast cancers [51], the aim of this work was to investigate the effects of HAS2-AS1 overexpression or silencing in regulating breast cancer cell line aggressiveness (i.e., viability, migration, and invasion).

Firstly, we decided to study the expression of HAS2-AS1 in a panel of three ER/PR positive and four triple-negative breast cancer cell lines and HBL100, which was used as a non-cancerous control cell line. As shown in Fig. 1A, HAS2-AS1 transcript levels, tested through quantitative RT-qPCR, were higher in TNBC cell lines with respect to ER/PR/HER2 positive cell lines. We obtained similar results taking advantage of the Cancer Cell Line Encyclopedia from the Broad Institute and Novartis, 2019 update [52]. We downloaded the HAS2-AS1 expression values from the cBioPortal database and analyzed the data using GraphPad Prism Software, finding a higher expression in ER-negative to ER-positive invasive breast cancer cell lines (Supplemental Fig. 1A).

We also investigated HAS2-AS1 expression in breast cancer tissues by using data from the Cancer Genome Atlas (TCGA) Breast Invasive Carcinoma Project [52]. We found that the HAS2-AS1 transcript levels were significantly higher in ER-negative compared to ER-positive samples (Fig. 1B). Additionally, survival analysis of the same TCGA dataset showed no statistically significant correlation between HAS2-AS1 expression and overall survival in patients with ER-positive breast cancer (Fig. 1C). In contrast, HAS2-AS1 expression was found to be positively correlated with overall survival of ER-negative breast cancer patients (Fig. 1D).

These results suggest that there was a different expression of HAS2-AS1 in breast cancer cell lines and tissues highlighting a higher expression in TNBC cell lines and ER-negative cancer tissues. Moreover, an elevated HAS2-AS1 expression in ER-negative cancer tissues was correlated to higher survival of patients.

HAS2-AS1 modulates cell viability in TNBC cell lines but not in ER-positive cell lines

To investigate the possible effect of HAS2-AS1 modulation on cell viability, we measured cell viability by 3-(4,5-dimethylthiazol-2-yl)-2,5-diphenyltetrazolium bromide (MTT) assay comparing four breast cancer cell lines that are routinely used as a model of aggressive TNBC (MDA-MB-231 and Hs 578T) or non-aggressive ER-positive cancers (MCF-7 and T-47D). In MCF-7 cells the transient HAS2-AS1 siRNA silencing obtained by transfecting 50 nM siRNA against HAS2-AS1 (Fig. 2A), did not affect cell viability. Similar results were obtained by overexpressing the full length (FL) or the short (S) and long (L) isoforms of HAS2-AS1 (Fig. 2B and C). Comparable data on cell viability were observed on the other non-aggressive ER-positive cell line T-47D (Supplemental Fig. 2A, B).

When testing cell viability on the aggressive triple-negative MDA-MB-231 cell line, we found that the transient silencing of HAS2-AS1 doubled cell viability with respect to the control cells transfected with scrambled siRNA (Fig. 2D). Interestingly, MDA-MB-231 cells transfected to overexpress HAS2-AS1 FL (Fig. 2E) or the S or L isoforms of exon 2 (Fig. 2F) showed a statistically significant reduction of viability with respect to the control cells transfected with the empty vectors. Interestingly, this biological effect seems to be dependent on the length of the two isoforms, as the transfection of the construct coding for the L isoform has a stronger inhibitory effect than the S isoform.

We also tested the aggressive ER-negative cell line Hs 578T, finding that the viability after HAS2-AS1 silencing was unaltered with respect to MDA-

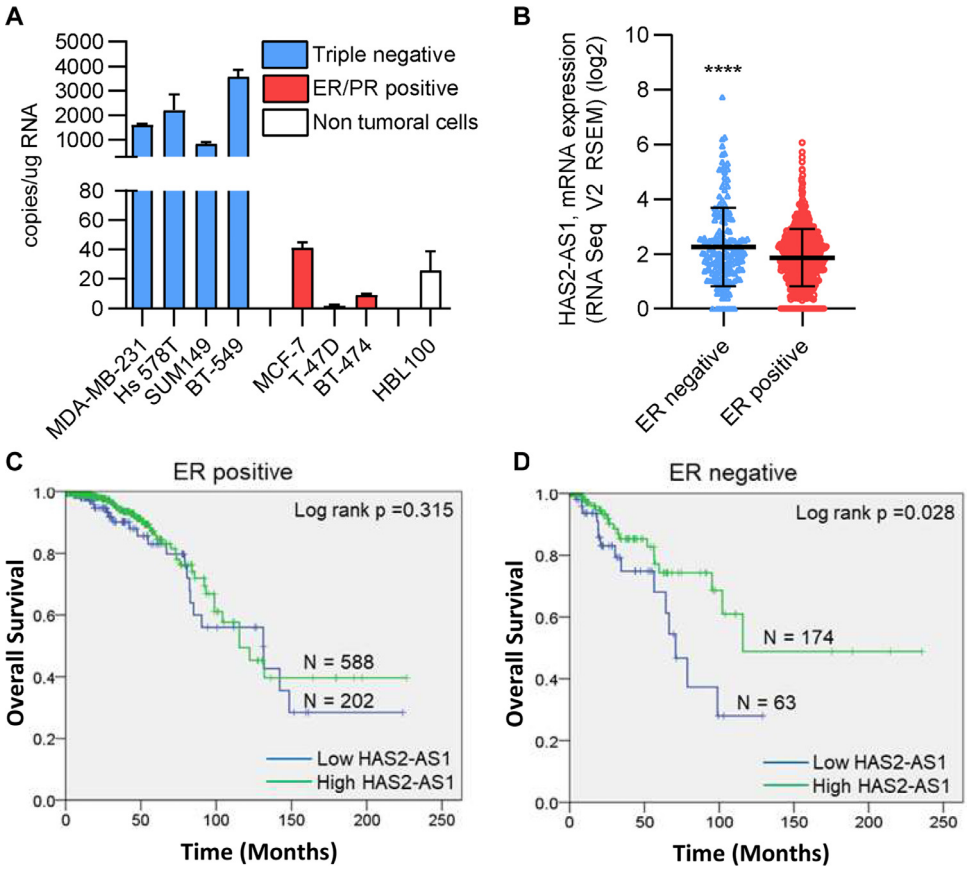

Fig. 1. HAS2-AS1 is highly expressed in triple-negative breast cancer cells and associated with a good prognosis in ER-negative breast cancer. (A) Absolute quantification of HAS2-AS1 copy numbers in triple-negative (blue) and ER/PR positive (red) breast cancer cell lines. The white bar represents the transformed but non-tumoral cell line HBL 100. Data are expressed as mean ± SEM of triplicates of three independent experiments. **(B)** Unpaired analysis of HAS2-AS1 gene expression in patient samples derived from invasive breast carcinomas (TCGA-BRCA gene expression data, cBioPortal.org), stratified for ER expression. ****, $p < 0.0001$. Data are expressed as mean±S.E.M. Kaplan Meier survival analysis of either ER-positive **(C)** or ER-negative **(D)** TCGA-BRCA breast cancer tissues. A cut off of HAS2-AS1 expression at the 25th percentile was applied.

MB-231. Interestingly, after HAS2-AS1 overexpression cell viability decreased, as in MDA-MB-231, althought to a lower extent.

These results suggest that the modulation of HAS2-AS1 expression levels affected the viability only of aggressive TNBC cell lines. Further, HAS2-AS1 transient silencing or overexpression in ER-negative cell lines induced an increase or a decrease of cell viability, respectively.

HAS2-AS1 influences motility and polarity of aggressive TNBC cell lines

The evaluation of cell migration was performed in the T-47D, MDA-MB-231, and Hs 578T cell lines by a 2D scratch assay, known also as wound healing assay, in the presence of 0.1% fetal bovine serum (FBS) to reduce cell proliferation. Fig. 3A shows that the transient silencing of HAS2-AS1 in the aggressive TNBC MDA-MB-231 cell line increased cell migration to a confluent monolayer compared to control cells. On the contrary, the transient overexpression of the FL isoform of HAS2-AS1 or the transient overexpression of S or L isoforms of exon 2 of HAS2-AS1 significantly decreased cell migration (Fig. 3B, C). Similar results were obtained on the other aggressive TNBC Hs 578T cell line (Supplemental Fig. 3A, B).

The modulation of HAS2-AS1 expression in the non-aggressive ER-positive cell line T-47D, instead, did not significantly alter the migratory properties of the cells (Supplemental Fig. 3C, 3D).

Considering the lack of effects on the migration of ER-positive cell lines upon HAS2-AS1 modulation, to evaluate 3D cell motility we focused on MDA-MB-231 and performed a Matrigel cell invasion assay. As shown in Fig. 3D, the transient silencing of HAS2-AS1 dramatically increased cell invasive capabilities. As a control, we transiently silenced HAS2 by transfecting 50 nM of siRNA against

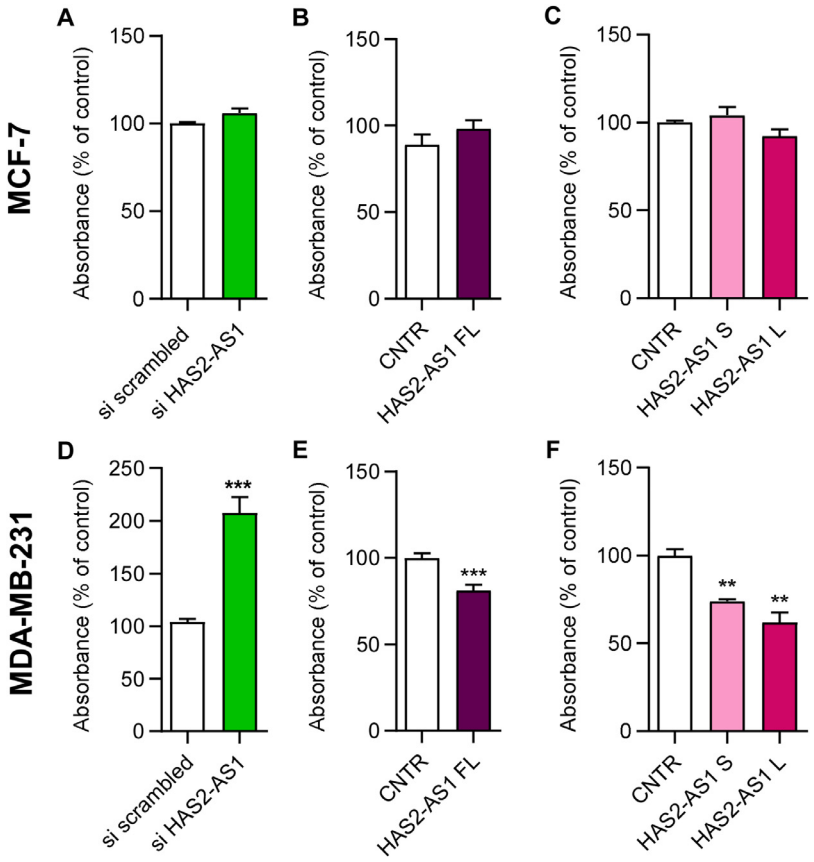

Fig. 2. HAS2-AS1 selectively inhibits cell viability in ER-negative breast cancer cells. (A) MTT assay performed in MCF-7 upon the transfection for 48 h of 50 nM HAS2-AS1 siRNA or relative scrambled control, or the transfection of 2 μg of **(B)** plasmid overexpressing HAS2-AS1 full-length or **(C)** pcDNA3 vector overexpressing exon 2 of HAS2-AS1 short (S) or long (L) isoforms with relative control empty vector (CNTR). MDA-MB-231 viability tested through MTT assay after the **(D)** transfection of 50 nM HAS2-AS1 siRNA or the transfection of 2 μg of plasmid overexpressing HAS2-AS1 **(E)** full length or **(F)** the S or the L isoforms of exon 2 with relative empty control vectors. All the experiments were conducted four times in triplicates. Data are expressed as mean±S.E.M. **,$p < 0.01$; ***,$p < 0.001$.

HAS2, which is known to promote motility and, as expected, the invasion capabilities of the cells were significantly reduced. On the contrary, when MDA-MB-231 cells were transiently transfected with constructs overexpressing the S or L isoforms of exon 2 of HAS2-AS1 their invasive capabilities were significantly reduced (Fig. 3E).

Since cell shape is related to the ability of a cell to move, we performed morphometric analyses of MDA-MB-231 cells that were in scratch area 24 h after the removing of the cell with a pipette tip. Cells were stained with DiI (Fig. 4A, B, C) and the long and the short axis of cells were measured via NIH ImageJ software (Fig. 4D). As expected HAS2-AS1 silenced cells, that showed high migratory capabilities, had a greater long:short axis ratio, whereas HAS2-AS1 overexpressing cells had a lower long: short axis ratio, suggesting a roundish shape typical of non-moving cells similar to those silenced for HAS2 (Fig. 4 E, F, and G).

These results indicate that the modulation of HAS2-AS1 influenced the motility of TNBC cell lines.

HAS2-AS1 does not alter HA levels and HAS2 expression in MDA-MB-231 cells

HAS2-AS1 is known to regulate HAS2 expression and, consequently, HA deposition which is often associated with cancer progression and metastasis [41,53]. To test whether HAS2-AS1 modulation could alter HA production in MDA-MB-231 cells, we measured the levels of HA released in the culture medium by ELISA and quantified HA contained in the pericellular matrix by particle exclusion assay and flow cytometry. As shown in Fig. 5A, the transient silencing of HAS2-AS1 did not alter the amount of HA released in the culture medium. As a control experiment, we transiently silenced HAS2 and found a significant reduction of HA released in the

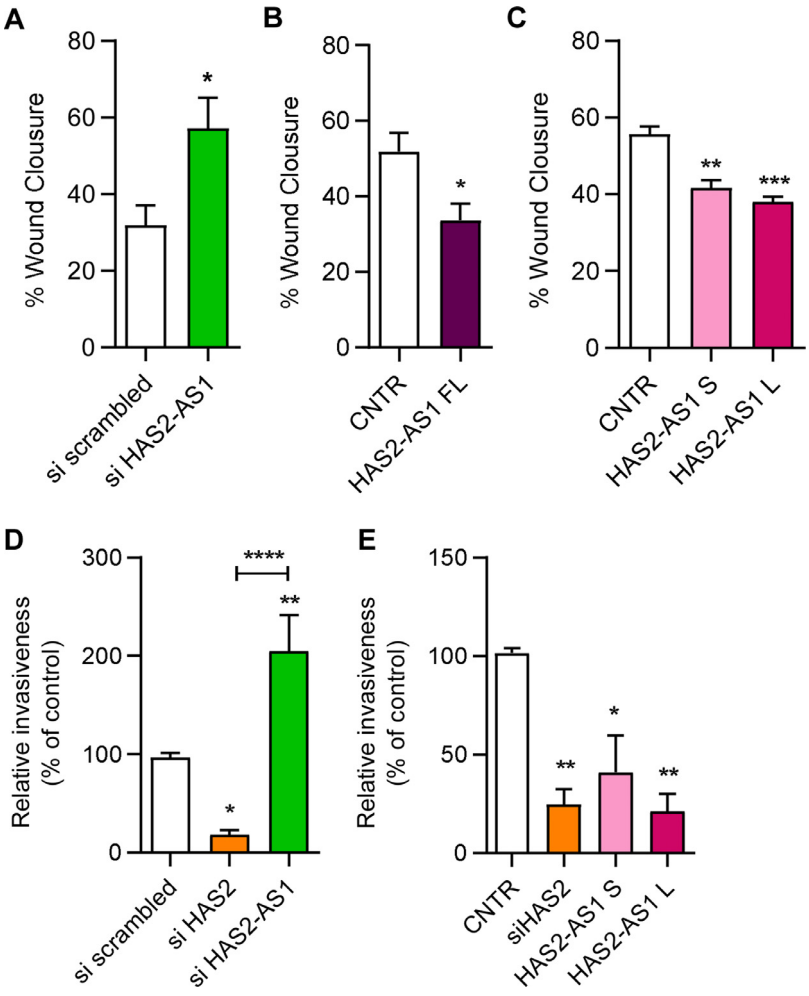

Fig. 3. HAS2-AS1 inhibits breast cancer cell motility and invasiveness. (A) Scratch assay performed in MDA-MB-231 after the transfection of 50 nM HAS2-AS1 siRNA or scrambled control for 48 h. **(B)** Scratch assay upon MDA-MB-231 transfection for 48 h with 2 μg of plasmid overexpressing HAS2-AS1 full length or **(C)** the S or the L isoforms of exon 2 or relative control empty vectors. Data were analysed using the free software TScratch and represented as mean ± SEM of five independent experiments. Bars represent the % of wound closure after 24 h of migration in absence of serum and are normalized on the initial wound area at time 0. *,$p < 0.5$. **(D)** Matrigel invasion assay performed in MDA-MB-231 after the transfection of 50 nM siRNA against HAS2-AS1 or HAS2 or scrambled control for 48 h. **(E)** Matrigel invasion assay upon MDA-MB-231 transfection for 48 h with 2 μg of vectors overexpressing HAS2-AS1 S or L isoforms of exon 2 or relative empty control vector. As a control, MDA-MB-231 cells were silenced for HAS2 using 50 nM of target siRNA. Data are represented as relative invasiveness of control and displayed as mean ± SEM of eight independent experiments. *,$p < 0.5$; **,$p < 0.01$;***,$p < 0.001$; ****,$p < 0.0001$.

conditioned medium. Similarly, also the transient transfection of the S or L isoforms of exon 2 of HAS2-AS1 did not alter the amount of HA released into the conditioned medium (Fig. 5B). Further, HAS2-AS1 transient silencing did not change HA associated with the cell layer (i.e., pericellular matrix) as measured in Fig. 5C. As a control experiment, we transiently silenced HAS2 and degraded the HA with hyaluronidase, finding significant reductions of the pericellular matrix suggesting that the method we used was reliable. To further confirm these data, we stained pericellular HA with FITC labelled HA binding protein (HABP) and quantified fluorescence by flow cytometry. As shown in Fig. 5D, E, F, and G the mean fluorescence intensity did not change after the transient silencing HAS2-AS1 or the overexpression of the S or L isoform of exon 2 of HAS2-AS1.

These data are quite surprising as it is known that HAS2-AS1 can regulate the expression of HAS2 which is responsible for HA production. Therefore, we measure by quantitative RT-qPCR the expression of HASes after HAS2-AS1 modulation in MDA-MB-231. In untreated MDA-MB-231 cells, HAS1 was not detectable whereas HAS2 was about 35-fold more expressed than HAS3 (Supplemental Fig.

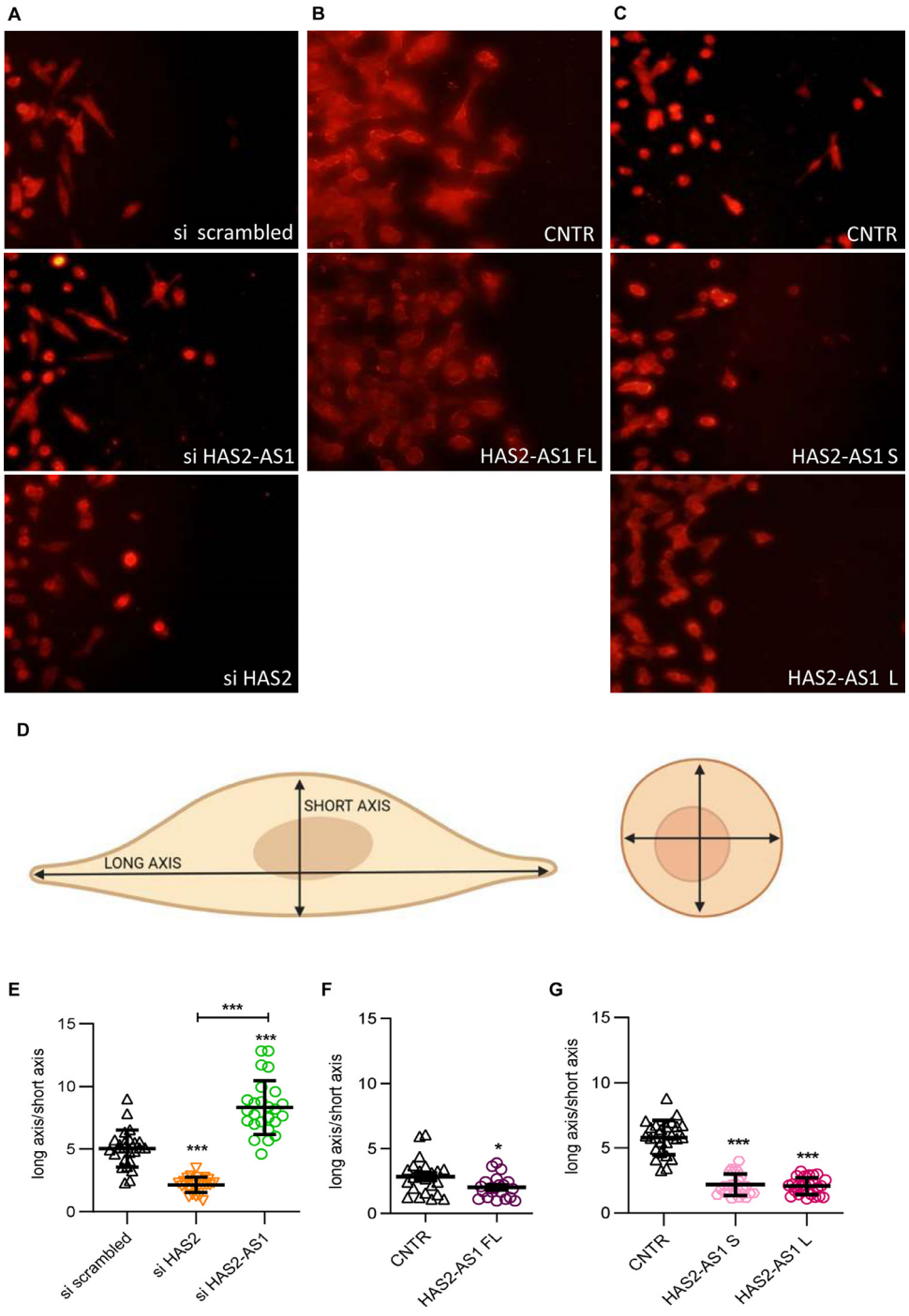

Fig. 4. HAS2-AS1 reduces the tumorigenic phenotypes of ER-negative breast cancer cells. (A) MDA-MB-231 cell morphology 24 h after scratch assay. Cells were transfected with 50 nM siRNA against HAS2-AS1 or HAS2 or scrambled control for 48 h. Magnification 200X. **(B)** MDA-MB-231 cell morphology 24 h after scratch assay. Cells were transfected for 48 h with 2 μg of plasmid overexpressing HAS2-AS1 full length or **(C)** pcDNA3 vector overexpressing exon 2 of HAS2-AS1 S or L isoforms, with relative empty control vectors. Magnification 200X. **(D)** Scheme representing how the cell morphology measures (i.e., short and long axis) were taken from images in panels A, B, and C by using ImageJ software . **(E)** Quantification of cell morphology changes measuring long axis:short axis ratio in MDA-MB-231 cells in A panels. **(F)** Quantification of cell morphology changes measuring long axis:short axis ratio in MDA-MB-231 cells in B panels. **(G)** Quantification of cell morphology changes measuring long axis:short axis ratio in MDA-MB-231 cells in C panels. Data are expressed as mean±S.E.M. *,$p < 0.5$; ***,$p < 0.001$.

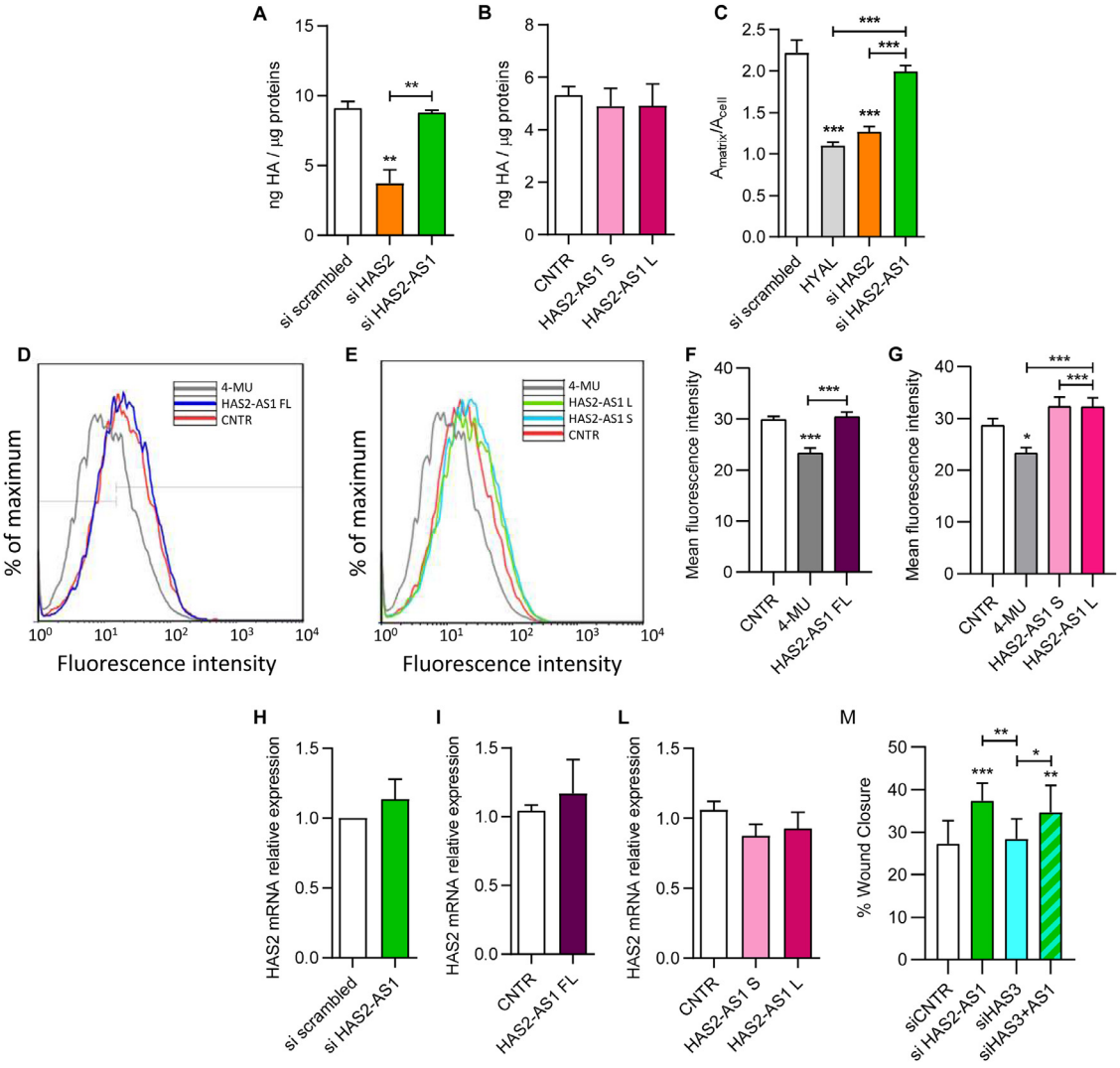

Fig. 5. HAS2-AS1 expression does not alter HA synthesis in the TNBC model cell line MDA-MB-231. (A) Determination by ELISA assay of the HA content in culture media of MDA-MB-231 transfected for 48 h with 50 nM siRNA against HAS2, HAS2-AS1 or scrambled siRNA. Results are expressed as mean of three independent experiments ± SEM. **,$p < 0.01$. **(B)** HA quantification by ELISA assay of MDA-MB-231 culture media after the transfection with 2 µg of a plasmid encoding for HAS2-AS1 S or HAS2-AS1 L isoforms of exon 2 or relative empty control vector. Results are expressed as mean of three independent experiments ± SEM, normalized to the µg of extracted proteins and reported as % of the control. **(C)** Particle exclusion assay of MDA-MB-231 pericellular space. Cells were transfected for 48 h with 50 nM siRNA against HAS2, HAS2-AS1,scrambled siRNA or treated with 2 U/ml bovine hyaluronidase. Data are shown as mean ± SEM of three independent experiments. Results are expressed as the ratio between the area of ECM delimited by red blood cells and the area of the cell by using ImageJ software. ***,$p < 0.001$. **(D)** Pericellular amount of HA detected by flow cytometry using the FITC labelled hyaluronan binding protein (HABP) in MDA-MB-231 transfected with 2 µg of a plasmid coding for HAS2-AS1 full length (blue histogram) or empty control vector (red histogram). Cells were also treated with 1 µM 4-MU as a control (grey histogram). **(E)** Pericellular amount of HA detected by flow cytometry using the FITC labelled HABP in MDA-MB-231 transfected with 2 µg of a plasmid coding for HAS2-AS1 S (light blue histogram), HAS2-AS1 L (green histogram) or empty control vector (red histogram). Cells were also treated with 1 µM 4-MU as a control (grey histogram). **(F)** Quantified mean fluorescence intensity of histogram D. **(G)** Quantified mean fluorescence intensity of histogram E. **(H)** Quantitative RT-PCR showing HAS2 expression in MDA-MB-231 silenced for 48 h with 50 nM siRNA against HAS2-AS1 or siRNA scrambled control. Data are displayed as mean ± SEM of four independent experiments. **(I)** Quantitative RT-PCR analysis of HAS2 mRNA levels upon transfection of 2 µg of plasmids coding for HAS2-AS1 full length or **(L)** HAS2-AS1 S and HAS2-AS1 L. Bars represent mean ± SEM of four independent experiments. (**M**) Scratch assay performed on MDA-MB-231 cells after the transfection of 50 nM of siRNA against HAS2-AS1, HAS3, both HAS2-AS1 and HAS3 or scrambled control for 48 h. Bars represent the % of wound closure after 24 h of migration in absence of serum and are normalized on the initial wound area at time 0. Data were analysed using the free software TScratch and represented as mean ± SEM of four independent experiments. *, $p < 0.5$; **,$p < 0.01$; ***, $p < 0.001$.

4A). After the transient silencing of HAS2-AS1 (Fig. 5H) or overexpression of the FL (Fig. 5I), S or L isoforms of exon 2 of HAS2-AS1 (Fig. 5L), the amount of transcript coding for HAS2 remained at control levels. The overexpression of the FL or S or L isoforms of exon 2 of HAS2-AS1 did not alter the expression of HAS3 (Supplemental Fig. 4B, C). The transient silencing HAS2-AS1 induced a significant increase of about 3-fold of HAS3 (Supplemental Fig. 4D). However, as shown in Fig. 5M, no alteration in migration capabilities was detected upon HAS3 silencing. Moreover, after simultaneous silenging of HAS3 and HAS2-AS1, the observed increase in cell mobility is comparable to that of HAS2-AS1 silencing alone and, on the other hand, significantly different from HAS3 silencing. These results surprisingly indicate that in MDA-MB-231 the modulation of HAS2-AS1 neither altered the accumulation of HA nor the expression of HAS2.

Characterization of stable clones overexpressing the L isoform of exon 2 of HAS2-AS1

All the previous results have been obtained with transient transfections that can induce undesired effects as cellular stress due to the massive overexpression of the target gene or membrane damage due to lipofection. Therefore, we decided to produce stable MDA-MB-231 clones overexpressing the L isoform of exon 2 of HAS2-AS1. In fact, the transient transfection of this fragment of 256 bp (Supplemental Fig. 5) was able to significantly reduce MDA-MB-231 viability, migration, and invasion, showing a length-dependent stronger effect compared to the S isoform.

We selected two clones overexpressing L isoform of exon 2 of HAS2-AS1 (cl. LONG 1 and cl. LONG 2) and two control clones overexpressing the empty pcDNA3 cloning vector (cl. CNTR 3 and cl. CNTR 4). Both cl. LONG 1 and 2 expressed higher levels of HAS2-AS1 exon 2 compared to CNTR clones. Notably, cl. LONG 2 expressed almost twice as much HAS2-AS1 exon 2 transcript levels as cl. LONG 1 (Supplemental Fig. 6A).

During the preliminary characterization of the stable clones, we confirmed that, as observed after HAS2-AS1 L isoform transient overexpression (Fig. 5), cl. LONG 1 and 2 showed no differences in the amount of pericellular HA, even though a slight increase in HAS2 mRNA expression levels was seen in cl. LONG 1 and 2 with respect to control clones (Supplemental Fig. 6B, C). However, western blot analysis confirmed that no significant increase in HAS2 protein level was detectable among the four stable clones (Supplemental Fig. 6D, E).

Interestingly, cl. LONG 1 and 2 confirmed that HAS2-AS1 L isoform overexpression significantly reduces MDA-MB-231 motility compared to control clones (Supplemental Fig. 6F), showing even a more roundish epithelial-like phenotype with respect to the elongated mesenchymal-like phenotype of cl. CNTR 3 and 4 (Supplemental Fig. 6G, H).

The stability of HAS2-AS1 exon 2 L isoform overexpression in the selected clones allowed us to perform growth experiments spanning from seven to twenty days. Firstly, we evaluated the clonogenic abilities performing a 10 days 2D colony formation assay. Interestingly, cl. LONG 2 produced significantly fewer and smaller colonies than cl. CNTR 3 and 4 (Fig. 6A, Supplemental Fig. 6I). cl. LONG1, which expressed lower levels of HAS2-AS1 exon 2 with respect to cl. LONG 2, gave colonies similar to control clones.

Secondly, we tested the anchorage-independent cell growth abilities in soft agar. Again the cl. LONG 2 showed to be less prone to generate colonies, which also resulted significantly smaller in respect to cl. CNTR 3 and 4 (Fig. 6B, C). Further, cl. LONG 1 resulted to behave more similarly to cl. CNTRs than cl. LONG 2.

Eventually, to evaluate the effects of HAS2-AS1 L overexpression on cell proliferation, cell numbers for each stable clone were counted every 24 h for seven days, and live-cell numbers were used to generate a cell growth curve. As depicted in Fig. 6D, cl. LONG 2 appeared to be much less proliferative in comparison to control clones and even cl. LONG 1. Indeed, cl. LONG 2 had a mean population doubling of 3,12 compared to cl. LONG 1 with 4,85, cl. CNTR 3 with 4,68 and cl. CNTR 4 with 4,62 (data not shown).

These results on stable clones confirmed that high levels of HAS2-AS1 exon 2 reduced the tumorigenic phenotypes of MDA-MB231 cells, including migration, cell polarization, clonogenicity and growth. Interestingly, it appeared that the higher the overexpression levels of HAS2-AS1 L, the better the results in terms of tumor suppression, as cl. LONG 2 expressed almost twice as much HAS2-AS2 exon 2 L as cl. LONG 1.

Affymetrix microarray analysis of stable clones overexpressing the L isoform of exon 2 of HAS2-AS1

Given our discovery found that HA synthesis in MDA-MB-231 cells is not regulated by HAS2-AS1 (Fig. 4), we sought to investigate further into mechanistic pathways that may be effectively altered and regulated by this antisense transcript, cl. LONG 2 (the clone expressing higher levels of HAS2-AS1 exon 2 L isoform) and cl. CNTR 4 by transcriptome analysis using Affymetrix Clariom S microarrays. Genes that may be regulated by HAS2-AS1 were identified using the Transcriptome Analysis Control 4.0 software, applying the filtering criteria of fold

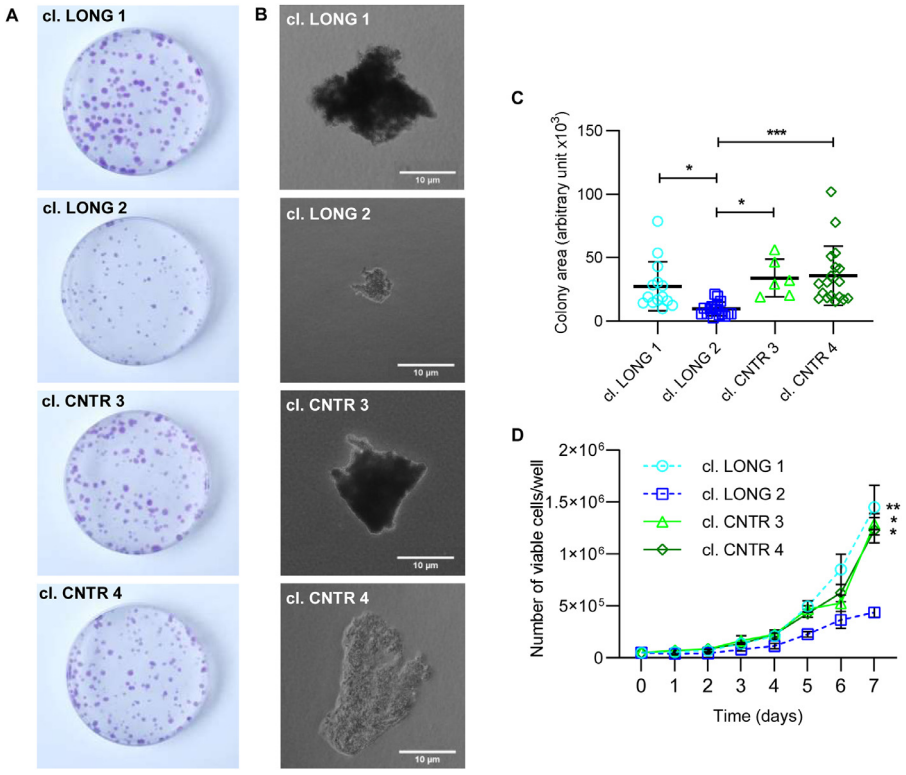

Fig. 6. Impact of HAS2-AS1 clone LONG2 on colony formation and cell viability. (A) Clonogenic assay of MDA-MB-231 stable clones overexpressing HAS2-AS1 L or empty vector at 10 days after seeding. **(B)** Soft-agar colony formation assay of MDA-MB-231 stable clones overexpressing HAS2-AS1 L or empty vector at 20 days after seeding. Magnification, 400X. **(C)** Quantification of soft-agar colony areas measured via ImageJ**.** Data are displayed as mean ± SEM. *, $p < 0.5$; ***,$p < 0.001$ **(D)** Growth curve of MDA-MB-231 stable clones overexpressing HAS2-AS1 L or empty vector. Values are reported as the average of three triplicates ± SEM. *,$p < 0.5$; **,$p < 0.01$.

change of 4-fold or higher and FDR p-value of below 0.05. In total, 366 unique genes were found to satisfy these criteria, of which 146 were upregulated and 220 were downregulated (Fig. 7A, Supplemental Table 1). The list of 366 genes were then uploaded into Database for Annotation, Visualization, and Integrated Discovery (DAVID) v6.8 for categorization according to their GOTERM BP functions (Fig. 7B, C). The lists of upregulated and downregulated genes with their corresponding functional categories are provided in Supplemental Tables 2 and 3, respectively.

We further analyzed the list of differentially expressed genes using the Kyoto Encyclopedia of Genes and Genomes (KEGG) to identify possible pathways that may be regulated by overexpression of HAS2-AS1. The pathways that were identified amongst the downregulated genes include (Fig. 7D): Transforming growth factor (TGF)-beta and chemokine signaling pathways, focal adhesion, ECM-receptor interaction, pathways in cancer and Phosphatidylinositol-3-Kinase and Protein Kinase B (PI3K-Akt) signaling pathway. In contrast, Jak-Stat signaling (with five associated genes) was the only pathway of upregulated genes found by KEGG analysis of the upregulated genes (data not shown).

Numerous genes associated with tumour-suppressive functions were identified in the upregulated list, as teneurin transmembrane protein 1 (TENM1), NCK associated protein 1 like (NCKAP1L), Cadherin 18 (CDH18) and interleukin 24 (IL24).

Among the most downregulated genes, we found the mRNAs coding for trefoil proteins (TFF1, 2 and 3) and epiregulin (EREG), the well-known Epidermal Growth Factor Receptor (EGFR) agonist. As this latter gene has a central role in tumorigenesis, we confirmed its expression via RT-qPCR finding that both HAS2-AS1 overexpressing clones, at different extent, showed decreased EREG levels (Fig. 7E).

Interestingly, raw Affymetrix Clariom S microarray data (data not shown) revealed a small but significant decrease of CD44 mRNA levels in cl. LONG 2 over cl. CNTR 4, with a fold change of -1.7 ($p < 0.0016$, FDR 0.0103), while no significant change were detected for RHAMM. CD44 downregulation in cl. LONG 2 was also confirmed via RT-qPCR analysis, as shown in Fig. 7F.

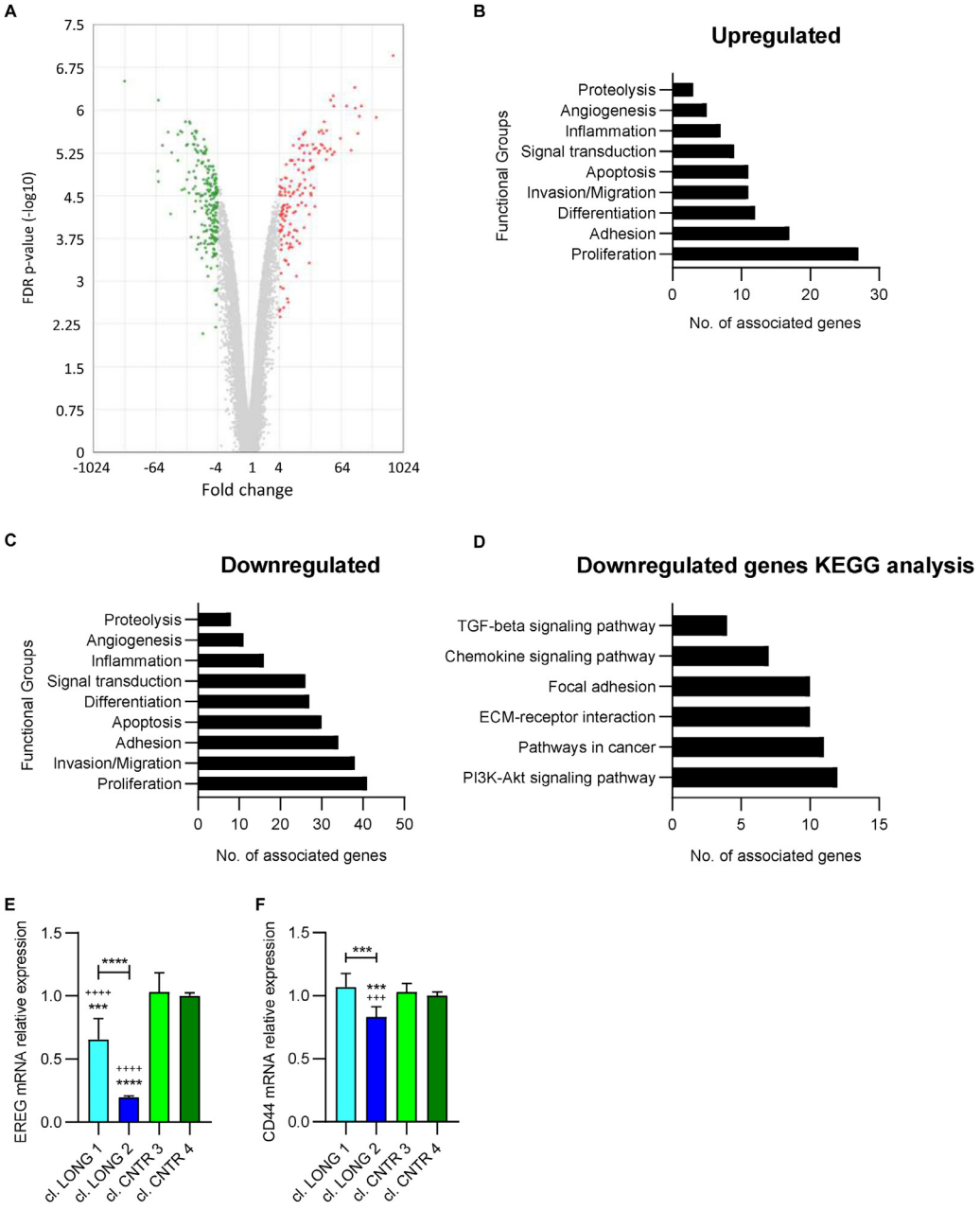

Fig. 7. Analysis of differentially expressed genes in cl. LONG 2 or control cl. CNTR 4. (A) Volcano plot of transcriptome comparison. Genes that were significantly up- or downregulated by at least 4-fold are shown in red or green, respectively. Statistical significance is defined as a false discovery rate (FDR) adjusted p-value of below 0.05. **(B)** Upregulated and **(C)** downregulated genes were uploaded onto DAVID and functionally sorted. **(D)** Several pathways were identified among the downregulated genes from KEGG analysis. **(E)** Quantitative RT-PCR analyses measuring EREG expression levels in in cl. LONG 1, cl. LONG 2 or control clones cl. CNTR 3 and cl. CNTR 4. Data are reported as mean ± S.E.M of three independent triplicates. ***, $p < 0.001$; ****, $p < 0.0001$. **(F)** Quantitative RT-PCR analyses measuring CD44 expression levels in in cl. LONG 1, cl. LONG 2 or control clones cl. CNTR 3 and cl. CNTR 4. Data are reported as mean ± S.E.M of three independent triplicates. ***, $p < 0.001$. * Represent significance with respect to cl. CNTR 4; + represent significance with respect to cl. CNTR 3.

HAS2-AS1 regulates EMT markers in MDA-MB-231 cells

The microarray results reported in Fig. 7 and in Supplemental Tables 2 and 3 clearly show that several genes involved in proliferation and motility were altered in agreement with our results on cell viability and invasivity. Moreover, the microarray identified many genes involved in adhesion; this finding is also supported by the alteration of cell

morphology induced by HAS2-AS1 overexpression (Fig. 4 and Supplemental Fig. 6). Further, HAS2-AS1 is known to regulate EMT via the TGFβ pathway in mouse mammary cells [51]. Therefore, to validate microarray data, we investigated the expression of EMT markers as vimentin, fibronectin, ZO-1 and Snai1 in the stable clones by qRT-PCR. In the two clones overexpressing the L isoform of exon 2 of HAS2-AS1 (cl. LONG 1 and 2) the expression of transcripts coding for vimentin, fibronectin and Snai1 was about 50% lower than in control clones (Fig. 8A). The expression of ZO-1 was slightly higher in the two exon 2 overexpressing clones respect to controls (Fig. 8A). Interestingly, the immunostaining of ZO-1 revealed the typical membrane localization of this tight junction marker in cl. LONG 1 and 2, whereas in control clones such membrane localization was not detectable (Fig. 8B). On the other hand, the mesenchymal marker fibronectin accumulated in control clones whereas cl. LONG 1 and cl. LONG2 showed a weak signal for fibronectin (Fig. 8B). Further, Western blotting analyses confirmed the lower fibronectin expression in the two clones that stably overexpress the L isoform of exon 2 of HAS2-AS1 respect to control clones (Fig. 8C).

These data confirm the microarray result on adhesion showing that the overexpression of the L isoform of exon 2 of HAS2-AS1 was able to alter the expression and localization of EMT markers favoring the less aggressive epithelial phenotype and thus promoting mesenchymal to epithelial transition (MET).

Discussion

Non-coding transcripts play a pivotal role in controlling gene expression. For example, miRNAs are known to interact with several target mRNAs with the consequence of deeply altering the landscape of gene expression [41]. Although belonging to the non-coding transcripts, up to now HAS2-AS1 was known to finely tune only the expression of its "cognate" gene *HAS2*. As HAS2 is the critical enzyme for HA synthesis, HAS2-AS1 has been described to profoundly affect ECM composition which, in turn, impacts many pathophysiological mechanisms as inflammation, cell motility, growth and survival. In fact, HAS2-AS1 has already been described in cumulus cell migration [43,54] hypoxic pulmonary hypertension [55], cardiovascular diseases [56–58] as well as in several cancers as brain tumors [46–48,59,60], lung cancers [50], ovarian cancer [49], oral carcinoma[45], osteosarcoma [44] in which, favoring HA deposition or interacting with miRNAs, enhances aggressiveness.

Breast cancer is one of the most prevalent malignancies in the world and it is widely described that its aggressiveness depends on ECM composition and HA [61]. Indeed, inhibition of HA synthesis or reduced HAS2 expression are known to decrease tumor aggressiveness, which is usually defined as the ability of a tumor cell to proliferate and migrate in the surrounding areas as well as to invade the basement membrane to originate metastasis. As aggressive breast tumors express high levels of HAS2-AS1 and this latter is known to modulate EMT in mouse mammary cells [51], our work aimed to investigate the role of this antisense transcript in two breast cancer subtypes, namely ER-positive and ER-negative. The TCGA-BRCA database showed that biopsies for patients with ER-positive cancers had a lower HAS2-AS1 expression with respect to ER-negative samples. This result was confirmed *in silico* on a panel of several breast cancer cell lines as well as in our experiments on well-known cellular models of ER-positive (ie., MCF-7 and T-47D) and ER-negative (i.e., MDA-MB-231 and Hs 578T) breast cancer cells. These results were somehow expected as a low HAS2-AS1 expression in low aggressive ER-positive samples could be responsible for the low HAS2 expression described in this type of breast cancer.

We further correlated HAS2-AS1 expression and the survival rate finding no correlation between the antisense expression and survival probability in ER-positive breast cancer. Surprisingly, in ER-negative tumors high HAS2-AS1 expression correlated with a high survival rate. This latter result was unexpected, as literature highlights that HAS2-AS1 facilitates HAS2 expression thus correlating with poor survival in several cancers [6]. However, it has to be considered that functional analyses of HAS2-AS1 were mainly based on studies in tumor cell lines, while the dataset analysis contains expression data from whole tumors which contain tumor cells, and stromal constituents (cancer-associated fibroblasts, tumor-infiltrating leukocytes, blodd vessels), which may have acted as a confounder. Furthermore, as discussed below, our transcriptomic analysis points out pathways different from HA synsthesis that could be mechanistically linked to novel functions of HAS2-AS1.

To better elucidate this point, we decided to investigate the role of HAS2-AS1 in well-known cellular models of ER-positive and ER-negative cancers, in which we easily manipulated the antisense expression by transient or stable transfections. In the two tested ER-positive cell lines neither the silencing nor the overexpression of HAS2-AS1 altered cell viability or migration, suggesting that the antisense was not involved in the control of cell aggressiveness. These data agree with cell survival rates, which are not affected by HAS2-AS1 in ER-positive breast cancer cell lines. Interestingly, in the two tested ER-negative cell lines the silencing of HAS2-AS1 increased cell viability, whereas the overexpression of the FL HAS2-AS1 or the isoforms L and S of the

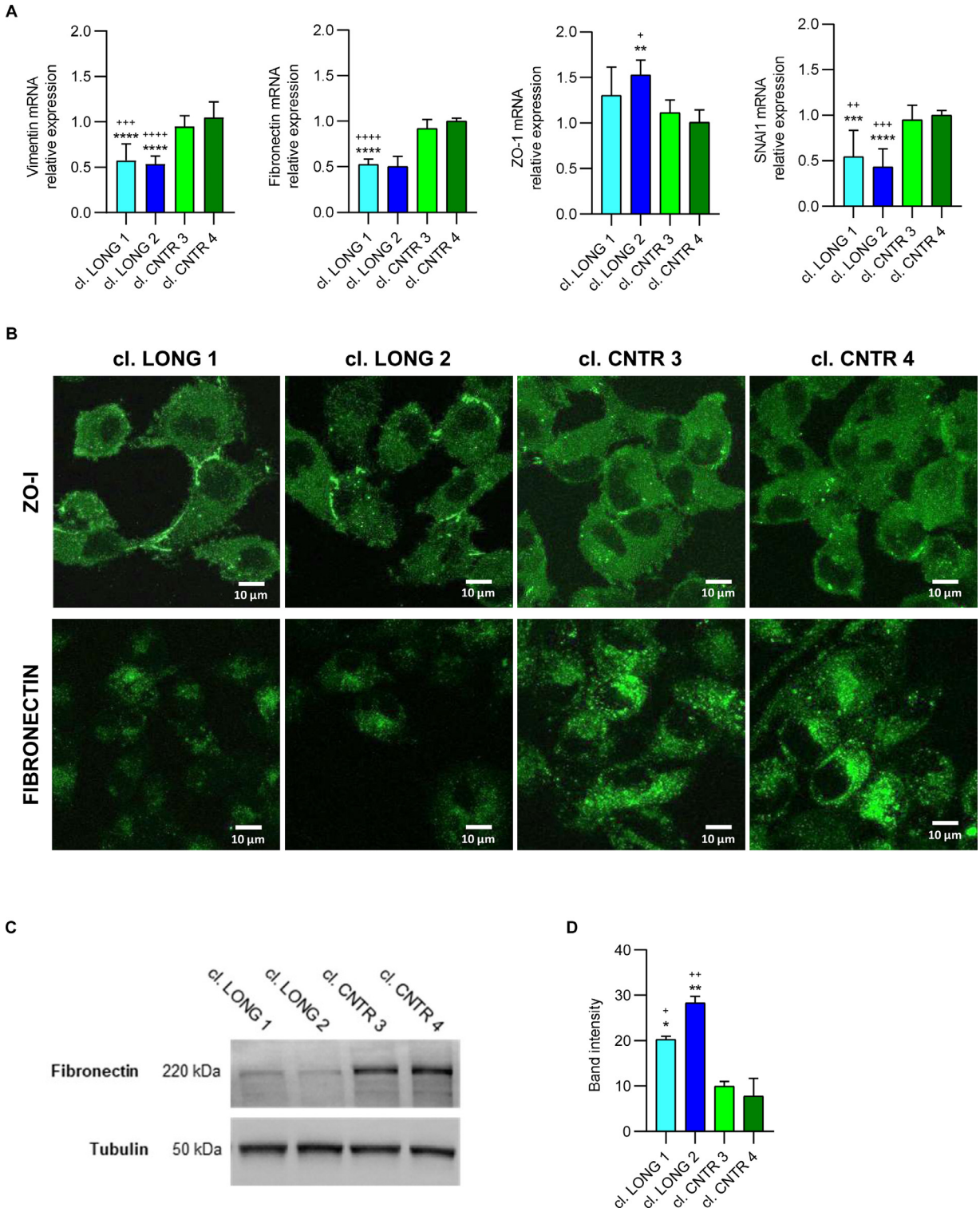

Fig. 8. Role of stable HAS2-AS1 exon 2 L isoform overexpression on MET. (A) RT-qPCR analyses measuring vimentin, fibronectin, ZO-1 or SNAI1 expression in MDA-MB-231 stable clones overexpressing the L isoform of HAS2-AS1 exon 2 (cl. LONG 1, cl. LONG 2) or empty control vectors (cl. CNTR 3 and cl. CNTR 4). Values are reported as the average of three independent triplicates ± SEM. **(B)** Representative confocal microscopy images of ZO-1 and fibronectin deposition in stable clones overexpressing the L isoform of HAS2-AS1 exon 2 (cl. LONG 1, cl. LONG 2) or empty control vectors (cl. CNTR 3 and cl. CNTR 4). Magnification 400X. **(C)** Representative Western blots of immunoreactive bands for fibronectin and tubulin from total protein extracts obtained from cl. LONG 1, cl. LONG 2 or control clones cl. CNTR 3 and

exon 2 of the antisense caused a significant decrease of cell viability, which is in line with the observed positive impact of HAS2-AS1 on patient prognosis. At this point, we decided to focus our attention on exon 2 of HAS2-AS1 as, being complementary to exon 1 of *HAS2* gene [43], we hypothesized having crucial functions to regulate *HAS2* transcription and HAS2 mRNA stability, as previously reported [42,43]. However, in the MDA-MB-231 cell line, HAS2-AS1 seems to regulate neither HAS2 expression nor HA deposition. This finding may serve to explain the initially surprising observation of improved survival of patients with high HAS2-AS1 expression as the beneficial effect may not be due to altered HA synthesis, but rather to independent mechanisms. Another possibility could be that HAS2-AS1 has effects on HA synthesis and HAS2 expresion (that may be not measurable with the techniques we employed) and that HAS2-AS1 may still have direct effects on other pathways.

Notably, the effects of the overexpression of the L isoform of exon 2 of HAS2-AS1 decreased cell aggressiveness to a higher extent than the S isoform. Even if we did not further investigate this point, we could speculate that the two isoforms of exon 2 of HAS2-AS1 could interact with different modulators as miRNAs. We performed *in silico* analyses to identify putative miRNAs interacting with the S or the L isoforms of exon 2 finding that the miRNA186-3p could have an additional binding site on the L isoform respect to the S isoform. As it has been already described that HAS2-AS1 could work as an endogenous competitor (ceRNA or sponge effect) for miR-466 [49] and miR-137 [47,62], the different effects of L and S isoforms could be ascribed to a different efficiency to sponge miRNA186-3p which is known to modulate cancer cell growth, motility and EMT [63−65].

The 2D migration (i.e., scratch assay), and the 3D invasion (i.e., through Matrigel) capabilities of the cells were also reduced after HAS2-AS1 overexpression. As motility is a characteristic of mesenchymal-like cells, which are characterized by a spindle-like aspect [66], we found that HAS2-AS1 overexpression in the tested ER-negative cell lines induced a change in the morphology from the spindle-like one of untreated MDA-MB-231 cells to a more roundish shape of HAS2-AS1 overexpressing cells. This spherical morphology is typical of epithelial cells that possess limited migratory capabilities [67]. This alteration could be a related to MET. Indeed our transcriptome analysis of KEGG pathways identified a downregulation of the TGF-beta pathway −a master regulator of EMT - in cl. LONG2 vs control cells, which may have induced a shift towards a less invasive, epithelial phenotype, as reported for glioma and mouse mammary epithelial cells [48,51]. Further, the experiments on stably transfected cells overexpressing the L isoform of exon 2 of HAS2-AS1 still confirmed that such overexpressing cells grew slowly and had a lower potential to form clones with respect to controls. Moreover, also CD44, a critical factor for stemness, is reduced in HAS2-AS1 overexpressing MDA-MB-231 clones, suggesting lower tumorigenic properties of the cells [68]. All these results clearly showed that HAS2-AS1 overexpression reduced the aggressiveness of ER-negative breast cancer cells. Moreover, this data agrees with the observed increased survival of patients affected by ER-negative breast cancers expressing high levels of HAS2-AS1.

We next started to explore the molecular mechanisms involved in the reduction of aggressiveness due to HAS2-AS1 (or only exon 2) overexpression in MDA-MB-231 cells, firstly checking HA and HAS2 expression. Surprisingly, all the three methods we used to quantify HA (i.e., ELISA, pericellular matrix measurement, and flow cytometry) indicated that HAS2-AS1 was not able to alter HA content in both stably transfected and transient overexpressing cells. Further, neither the mRNA expression nor the protein levels of HAS2, the main synthetic enzyme in MDA-MB-231, were affected by alterations of HAS2-AS1 expression levels. These results were surprising as it is well-known the strict relationship between HAS2-AS1 and its cognate gene product HAS2 that, in turn, regulates HA deposition [41]. Our research team was the first to characterize the role as chromatin organizer of HAS2-AS1 in the nucleus of human smooth muscle cells, describing its ability to modulate chromatin accessibility of *HAS2* promoter probably acting on histone post-translation modification as O-GlcNAcylation [42].

Although in different other tumor cell lines HAS2-AS1 sustains HAS2 expression [45,46,49,50], in MDA-MB-231 we found a different story suggesting the existence of different pathway(s) able to enhance HA synthesis, probably controlling directly the HAS2 promoter or HAS2 protein, which is known to have fine transcriptional and post-translational regulations [9,69,70]. The HAS2-AS1-independent HAS2 expression could be driven by the constitutive activation of several tyrosine kinase receptors, thus leading to the triggering of different intracellular

cl. CNTR 4. Numbers at the margins of the blots indicate relative molecular weights of the respective protein in kDa. **(D)** Relative band intensity of fibronectin immunoblotting. Values are expressed as mean ± SEM of 2 experiments of the percentage variation of the normalized O.D. obtained from each sample with respect to values obtained in cl. CNTR 4. *, $p < 0.5$; **, $p < 0.01$ ***, $p < 0.001$; ****, $p < 0.0001$. + represent significance in respect to cl. CNTR 3; * Represent significance in respect to cl. CNTR 4.

pathways as JAK-STAT, which, according to the microarray data, was found active in our HAS2-AS1 stable clones [71,72].

Since our results excluded that HAS2-AS1 could work via the canonical HAS2-HA axis, we decided to investigate via microarray analyses which mRNAs had an altered expression in stably transfected cells, to characterize the cellular pathways under the control of HAS2-AS1. We used the stable cl. LONG 2 that, having a higher exon 2 expression, showed reduced aggressiveness with respect to cl. LONG 1, whose behavior, instead, is more similar to control clones. Among the identified genes, several belong to the pathways modulating cell migration and proliferation, which agrees with the altered aggressiveness we observed in cl. LONG 2. Additionally, genes involved in cell adhesion have been enriched, which could justify the altered epithelial-like morphology of such cells. Interestingly, these analyses confirmed that no gene involved in HA synthesis (i.e., HASes) is regulated by HAS2-AS1 with the exception of the transcript coding for Cell Migration Inducing Hyaluronidase 1 (CEMIP) that has been identified to be significantly downregulated. As CEMIP is known to favor breast cancer cells growth and spreading [73], its reduced expression could contribute to the limited motility and viability of HAS2-AS1 overexpressing cells. Similarly, also the EREG messenger, which is well known to be involved in tumorigenesis and metabolic reprogramming [74,75], is downregulated in HAS2-AS1 overexpressing cells. Further, mRNAs coding for TFF1, 2 and 3 are among the most downregulated transcripts and these proteins are known to greatly induce breast cancer cell motility [76]. On the other hand, among the genes reported to be upregulated genes we found TENM1 transcripts involved in breast cancer better survival outcome [77] and NCKAP1L inhibiting breast cancer metastasis [77]. Interestingly, CDH18 has still a debated role in breast cancer but has been already demonstrated to be involved in the suppression of glioma cell invasiveness and correlate with prognosis of glioma patients [78]. Further, IL24, a well-studied tumor suppressor, is involved in diverse functions, including apoptosis, autophagy and suppression of metastasis [79–81].

These findings indicate for the first time that, at least in MDA-MB-231 cells, HAS2-AS1 can control several genes (not involved in HA synthesis) able to modulate different cellular pathways. Different hypotheses for further studies should be considered; first, the effect of this non-coding transcript to work as an epigenetic regulator in the nucleus allowing a reorganization of large portions of DNA forming peculiar looping interactions that have been implicated in gene regulation [82]. On the other hand, HAS2-AS1 could work as an endogenous competitor for miRNAs, as already described.

These new scenarios suggest that HAS2-AS1 can be involved in a more complex network of interactions that are critical for several cellular pathways. Nowadays lncRNAs are considered pivotal factors able to alter the landscape of gene expression in many tissues and several of them,such as EPB41L4A-AS2 and EGOT, have been described to inhibit breast cancer tumorigenesis [83]. In our opinion, HAS2-AS1 could be considered a new tumor suppressor specific for ER-negative breast cancer.

Materials and methods

Cell culture

MDA-MB-231, Hs 578T, BT-549 (high metastatic, triple-negative breast cancer cell lines) and HBL 100 cell lines (not diseased breast cells) were purchased by American Type Culture Collection (ATCC), grown, and maintained in complete Dulbecco's Modified Eagle Medium (DMEM) medium supplemented with 10% of FBS. SUM149 (high metastatic, triple-negative breast cancer cell lines) were purchased by ATCC, grown, and maintained in complete F-12 Nutrient Medium (Ham's F12) supplemented with 5% of heat-inactivated FBS, 10 mM HEPES, 1 μg/ml Hydrocortisone and 5 μg/ml Insulin. BT-474 (low metastatic, ERα-positive) were purchased by ATCC, grown, and maintained in complete DMEM:Ham's F12 (1:1 mixture) medium supplemented with 5% of FBS and 5 μg/ml Insulin. MCF-7 and T-47D (low metastatic, ERα-positive) breast cancer cell lines were obtained from ATCC and grown in complete Roswell Park Memorial Institute (RPMI) 1640 medium with 10% FBS. All cell lines were routinely harvested in a humidified 95% air/5% CO_2 incubator, at 37 °C.

Absolute HAS2-AS1 quantification via Real-Time qPCR

For the generation of the standard curve, pcDNA3.1-HAS2-AS1 L was obtained using Zymo-PURE II Plasmid Kits (#D4200, Zymo Research). A ten-fold dilution series over nine points were prepared from the plasmid DNA, starting from a dilution of 1.000.000 copies/μl to 1 copy/μl; then each dilution was used as a template for RT-qPCR, and amplified using HAS2-AS1 (Hs03309447_m1) TaqMan gene expression assays from Thermo Fisher Scientific. Each point was performed in triplicate. The standard curve was constructed by plotting Cq values against the logarithmic concentration of the calibrator plasmid.

Total RNAs were extracted and retrotranscribed as described below (see "RNA extraction and gene expression analysis"). The cDNA was analyzed for HAS2-AS1 expression via Taq Man gene

expression assays from Thermo Fisher Scientific (Hs03309447_m1) on Quantstudio 5 instrument (Applied Biosystems). The copies of HAS2-AS1 RNA molecules/μg of total RNA in the cell lines were obtained by interpolating the Cq values in the standard curve.

Bioinformatics analysis of HAS2-AS1 expression in breast cancer patients

Breast cancer data was extracted from the TCGA Research Network (https://www.cancer.gov/tcga) on 11th March 2021. Kaplan Meier survival analysis was conducted using SPSS version 22.0 (IBM Corp., Armonk, NY, USA). Eight of the 1,085 female patient datasets were excluded from the analysis as the HAS2-AS1 expression data was not available.

Cell transfection

Cells were plated in a 6-well plate and transfected with Lipofectamine 2000 Transfection Reagent (#11668027, ThermoFisher Scientific) following the manufacturer's instructions. Briefly, to transiently silence HAS2-AS1 expression, cells were transfected with 50 nM siRNA against HAS2-AS1 (Silencer® Select HAS2-AS1, #N265529, ThermoFisher Scientific), HAS2 (Silencer Pre-designed siRNA, #AM16708, ThermoFisher Scientific), HAS3 (HAS3, #AM16708, Thermo Fisher Scientific) or a scrambled siRNA (Silencer Negative Control #1, #AM4611, Thermo Fisher Scientific).

For subsequent determinations, 24−48 h after the transfections, cells were tested for silencing efficiency, by means of RT-qPCR, and only cells with a residual expression of the target genes lower than 25%, were used. To transiently overexpress the FL isoform of HAS2-AS1, 2 μg of the pLenti-GIII-CMV-GFP-2A-Puro overexpressing the sequence NR_002835 corresponding to human HAS2-AS1 (Abm) and, as a control, the same amount of pLenti-CMW-CMW-GFP-2A-Puro- Blank vector (Abm) were transfected for 48 h. To transiently overexpress the exon 2 L or S isoforms (Supplemental Fig. 6) of HAS2-AS1, 2 μg of a pcDNA3-HAS2-AS1 S or pcDNA3-HAS2-AS1 L [42] were transfected. As a control, the same amount of a pcDNA3 empty vector was transfected. Cells were used for subsequent determination 24−48 h after overexpression. At the end of each experimental determination, we confirmaed a reduced expresson of silenced genes (about 25% respect to controls) or an increased expression of overexpressed genes (at least 10-fold respect to controls).

Cell viability assay

To study cell viability upon HAS2-AS1 silencing or overexpression, a MTT (#20395, SERVA) assay was performed. Briefly, 8×10^3 cells were plated in a 96-well plate and transfected with lipofectamine following the manufacturer's instructions. 48 h after the transfection, cell culture medium was replaced with fresh medium supplemented with 50 μl of 5 mg/ml MTT and incubated at 37 °C for 5 h. The reaction was stopped by adding 200μl of DMSO and 25 μl of Sorensen glycine buffer per well. The plate was read at 570 nm.

Wound healing assay

To determine cell migration via bi-dimensional support, a wound-healing assay (also known as scratch assay) was performed. Twenty-four hours after the transfection, three scratches per well were done with a 20 μl pipette tip. Cells were washed twice with PBS and fresh medium with 0.1% FBS was added to each well, to minimize the proliferation component of cell migration. Pictures were taken at 0 and 24 h through light microscopy and analyzed by the TScratch software [84]. Results are presented as a percentage of wound closure.

Matrigel invasion chamber assay

The Matrigel invasion assay was performed to mimic tri-dimensional migration. Forty-eight hours after the transfection, $2{,}5 \times 10^5$ cells were seeded in each invasion filter (#354480, BD Biosciences) with complete medium. The day after, the medium was replaced with a free serum medium in the upper part of the chamber. The bottom of the well was filled with DMEM 10% FBS as a chemoattractant. After 18 h, the cells in the upper chamber were removed with a cotton swab and the ones on the lower surface were fixed and stained with Diff-Quik dye (#726443, Medion). Excised and mounted filter membranes were photographed using a Zeiss Axiovert microscope equipped with Axiovision software (Zeiss) at 100X magnifications. Five fields per image were counted. Relative invasiveness was expressed as a percentage of the number of cells versus the control.

Determination of cellular shape and polarity

Cells were stained with 5 μM 1,1′-Dioctadecyl-3,3,3′,3′-tetramethylindocarbocyanine perchlorate (DiI; #468495, SIGMA), kept 10 min at 37 °C, and finally 5 min at 4 °C. Subsequently, after washing the wells 5 times with PBS, pictures of the cells were taken through light microscopy and cell morphology was evaluated by measuring the long axis:short axis ratio of the cells by using Image J software [85].

HA quantifications

To detect the amount of HA after HAS2-AS1 silencing and overexpression, cell culture media were collected 48 h after the transfections and diluted 1:100. The quantification of HA was performed with the Hyaluronan quantikine ELISA kit (#DHYAL0, R&D Systems) according to the manufacturer's instructions.

To evaluate the pericellular coat of HA, a particle exclusion assay was performed. Briefly, 48 h after cells transfection, 1×10^6 fixed human red blood cells were washed in PBS and added to each well. After an incubation time of 30 min, cells were examined by contrast microscopy and 10 pictures per well were taken. As a control, cells were treated with 2U/ml of Hyaluronidase from *Streptomyces hyalurolyticus* (#H1136, SIGMA) or were transiently transfected with 50 nM siRNA against HAS2. The analysis of the images and the relative quantification was performed using the image analysis software ImageJ [85].

Cell surface HA was determined by cytofluorimetric analysis as described by Vitale et al. [86]. Briefly, 24 h after the transfection cells were detached and counted. 5×10^5 cells were washed 3 times in PBS and incubated with 5 μg of biotinylated hyaluronan binding protein (bHABP, # BC41, Hokudo) in 100 μl of cold PBS for 1 h at 4°C. Cells were then washed 3 times with 1 ml of PBS and centrifuged 5 min at 0.8g at 4°C. The supernatant was discarded, and cells were incubated with 1:100 FITC-streptavidin (#405202, Biolegend Campoverde) in cold PBS for 45 min at 4°C. After 3 washes, MDA-MB-231 were resuspended in 400 μl of PBS and analyzed by flow cytometry. As a control, cell were treated with 0,5 mM 4-MU.

RNA extraction and gene expression analysis

Total RNA was extracted by NucleoSpin RNA (#740955, MACHEREY-NAGEL), an RNA isolation kit containing a DNA digestion step. RNA samples were quantified with a NanoDrop (ThermoFisher, Life Technologies) and run on an agarose gel for quality control. Two μg of total RNA were then retrotranscribed using the High Capacity cDNA synthesis kit (#4368814, Applied Biosystems) and amplified on an ABI Prism 7000 instrument (Applied Biosystems). The cDNA was then analyzed using the following Taq Man gene expression assays from Thermo Fisher Scientific: HAS2-AS1 (Hs03309447_m1); HAS2 (Hs00193435_m1); HAS3 (Hs00193436_m1); CD44 (Hs01075861_m1); EREG (Hs00914313_m1) and β-actin (Hs99999903_m1). RT-qPCR was performed on a QuantStudio 3 Real-Time PCR Instrument (Thermo Fisher Scientific).

For stable clones screening and EMT determiantions, the SYBR Green PCR Master Mix (#4309155, Thermo Fisher Scientific) was used. The expression levels of target L isoform of exon 2 of HAS2-AS1 (FW: 5' TCTTGACTTCTCCTTCCCCG 3'; RV: 5' AAGTTGGAGGAGGCAGAAGG 3'), vimentin (FW: 5' TCGCAGAAAGGCACTTGAAAGC 3'; RV: 5' TCAGCATCACGATGACCTTGAA 3'), fibronectin (FW: 5' ACCGTGGGCAACTCTGTCAA 3'; RV: 5' CCCACTCATCTCCAACGGCA 3'), ZO-1 (FW: 5' GATGATGCCTCGTTCTAC 3'; RV: 5' GTGTTGTGGATACCTTGT 3') and SNAI1 (FW: 5' CCCGACAAGTGACAGCCATT 3'; RV: 5' CGAGCCCAGGCAGCTATTTC 3') were normalized to the expression levels of the reference gene *β-actin* (FW: 5' ACCAGTTCGCCATGGATGAC 3'; RV: 5' TGCCGGAGCCGTTGTC 3') and relative normalized expression was calculated based on the $\Delta\Delta C_t$ method.

Stable cell lines generation

MDA-MB-231 cells were plated onto 6-well plates and cultured for 24 h at a final confluence of 85%. On the next day, cells were transfected using Lipofectamine 2000 Transfection Reagent (#11668027, Thermo Fisher Scientific) with 2 μg of pcDNA3-HAS2-AS1 L or pcDNA3 empty vector. Twenty-four hours after transfection, cells were split into five 96-well plates at a concentration of 0,4 cells/well, selected in 800 μg/ml G-418 (#G8168, Sigma-Aldrich) and expanded. Clones were then screened for their exon 2 of HAS2-AS1 L isoform expression levels, via RT-qPCR (see "RNA extraction and gene expression analysis" for details).

Western immunoblot analyses

Cells were lysed in RIPA buffer (50 mM Tris-HCl, pH 8.0, 150 mM NaCl, 1% NP-40, 0.1% sodium dodecyl sulfate, 0.5% sodium deoxycholate), supplemented with Protease/Phopsphatase inhibitor (#5872, Cell Signaling Technology) and protein concentration was measured by Quantum Protein BCA assay (#EMP014500, Euroclone). Equal amounts of protein samples were subjected to SDS-polyacrylamide gel electrophoresis, followed by semi-dry transfer to nitrocellulose membrane using Trans-Blot Turbo Transfer System (Biorad) and blocking in 4% bovine serum albumin in Tris-buffered saline, supplemented with 1% Tween-20. Subsequently, the membranes were incubated with HAS2 (1:700; #34067, Santa Cruz Biotechnology) or fibronectin (1:20000; #F3648, Sigma-Aldrich) primary antibody at 4°C overnight, followed by incubation with anti-horseradish peroxidase-conjugated secondary antibodies (1:10000; #2354, Santa Cruz Biotechnology) for 1 h at room temperature. The antibody/substrate complex was visualized by chemiluminescence using a chemiluminescence kit (LiteAblot TURBO,

#EMP012001, Euroclone). Images were taken by Alliance Q9 Mini instrument (Uvitec) and signal intensity was evaluated using NineAlliance software (Uvitec). Tubulin (#135659, Santa Cruz Biotechnology) was used as the protein loading control. HAS2 or fibronectin protein levels were expressed as the percentage variation of the optical density (expressed in arbitrary units) of the signal normalized to the respective tubulin in treated cells compared to the controls.

Clonogenic formation assay

MDA-MB-231 stable clones overexpressing exon 2 of HAS2-AS1 L isoform or pcDNA3 empty vector were seeded in 60 mm plates (500 cells/well) and cultured for 10 days. The culture medium was replaced with fresh medium every 3 days. The colonies were fixed and stained with 0,1% crystal violet, washed extensively to remove excess dye, and imaged.

Anchorage-independent colony formation assay in soft agar

Soft agar plates were prepared by pouring in a 12 multi-well plate a feeding underlay layer and a growth overlay. To prepare the underlay, complete DMEM added with 20% FBS and 800 μg/ml G418 was mixed with Difco Noble Agar (#214230, BD Bioscience) at a final concentration of 0,6%. The plate was kept for 1 h at room temperature and then overnight at 37 °C to solidify and equilibrate. The day after, 1000 cells/well were resuspended in complete DMEM added with 20% FBS and 800 μg/ml G418 (#G8168, Sigma-Aldrich) and mixed with Noble Agar, at a final concentration of 0,3%. The plate was kept for 1 h at room temperature and then overnight at 37 °C to solidify and equilibrate. Cells were let grow for 20 days, and then images of colonies were taken under a light microscope (Olympus) at 400X magnification. Colonies areas were measured with ImageJ software [85].

Growth curve

The growth curve was characterized by measuring the number of cells for 7 consecutive days at 24 h intervals. MDA-MB-231 stable clones overexpressing HAS2-AS1 L or pcDNA empty vector were seeded in a 6-well plate at an initial concentration of 5×104 cells/well and cultured in complete DMEM with 10% FBS and 800 μg/ml G418 (#G8168, Sigma-Aldrich). The culture medium was replaced with fresh one every day. Every 24 h, cells were harvested using 0,5% trypsin, diluted with a 0,4% trypan blue working solution and counted with a Bürker counting chamber. Each sample was measured three times, in triplicates. Cell-growth curves were drawn from living cells numbers.

Transcriptome analysis of stable MDA-MB-231 cells overexpressing HAS2-AS1 exon 2 L

Total RNA was extracted from cultured cells using the Direct-zol RNA Kit (Zymo Research Corporation, Irvine, CA, USA) and processed for hybridization to the Affymetrix Clariom S Human Arrays (Affymetrix., Santa Clara, CA., USA) according to the respective manufacturers' protocols. The CEL files were analyzed using the Transcriptome Analysis Console 4.0 Software (Affymetrix). After Robust Multiarray Average (RMA) normalization, differentially expressed genes with 4-fold or greater changes were identified with statistical significance defined by a false discovery rate (FDR) adjusted p-value of below 0.05. The list of genes was further analyzed using DAVID v6.8 and classified into associated functional groups and KEGG pathways.

Immunofluorescence staining

For immunofluorescence staining, MDA-MB-231 stable clones overexpressing exon 2 of HAS2-AS1 L isoform or pcDNA3 empty vector were seeded in a 12-well plate upon glass microscopy dishes and allowed to settle for 24 h at 37 °C. Then, cells were fixed for 30 min in 4% paraformaldehyde, followed by 15 min permeabilization in 0.1% Triton X-100, blocking for 60 min in 1% BSA in PBS, and incubation overnight at 4 °C with the primary antibodies against ZO-1 (1:200, #33-9100, Life Technologies) or fibronectin (1:1000, # F3648, Sigma-Aldrich).

Then cells were incubated with secondary FITC-conjugated antibodies (1:1000) for 1 h at room temperature in the dark. Extensive washes with 1% BSA in PBS were performed between the aforementioned steps. Subsequently, coverslips were set onto glass slides and mounted by using 10 μl of VectaShield HardSet mounting medium containing 4′,6′-diamidino-2-phenylindole (DAPI, Vector Laboratories) for nuclear visualization. Finally, images were taken using a confocal microscope (Leica TCS SP5, Wetzlar, Germany).

Statistical analysis

All experiments were repeated at least three times in duplicates, if not differently indicated. Data are shown as the mean values ±SEM. The data were tested for significance employing the one-way Analysis of Variances (ANOVA) test followed by Tukey's post hoc test to identify differences between the means. Statistical comparison between two groups was made using an unpaired Student's t-test. The level of significance was set at $p < 0.05$.

Acknowledgements

This work was supported by the MIUR Grant PRIN 2017T8CMCY (to E. K.), the University of Insubria FAR (to D.V., A.P., M.V., and E.K.) and the EU H2020 Marie Skłodowska-Curie Grant 645756 "GLYCANC" (to A.P., M.G.), and the National Medical Research Council Grant MOH-000152 (to G.W. Y.). Ar.P. is a PhD student of the "Life Science and Biotechnology" course the University of Insubria. We gratefully acknowledge the "Centro Grandi Attrezzature per la Ricerca Biomedica" Università degli Studi dell'Insubria, for instruments facility (confocal microscopy). We are grateful to Tim Bowen from the University of Cardiff (UK) for providing us with the plasmids expressing the short and long isoforms of exon 2 of HAS2-AS1.

Supplementary materials

Supplementary material associated with this article can be found in the online version at doi:10.1016/j.matbio.2022.03.009.

Received 15 October 2021;
Received in revised form 8 March 2022;
Accepted 31 March 2022
Available online 6 April 2022

Keywords:
Extracellular matrix;
HAS2-AS1;
Non-coding RNA;
Tumor suppressor;
HAS2;
Hyaluronan;
Proteoglycans;
Aggressiveness;
Tumorigenicity;
Survival

Abbreviations:
4-MU, 4-methylumbelliferone; ANOVA, analysis of variance; ATCC, American Type Culture Collection; CDH18, Cadherin 18; CEMIP, Cell Migration Inducing Hyaluronidase 1; DAVID, Database for Annotation, Visualization, and Integrated Discovery; DMEM, Dulbecco's modified Eagle's medium; ECM, extracellular matrix; EGFR, Epithelial Growth Factor Receptor; EMT, Epithelial to mesenchymal transition; ER, estrogen receptor; EREG, Epiregulin; ERK, extracellular signal-regulated kinases; FBS, Fetal Bovine serum; FDR, false discovery rate; GlcNAc, N-acetyl-glucosamine; GlcUA, Glucuronic acid; HA, hyaluronan; HABP, hyaluronan binding protein; Ham's F12, F-12 Nutrient Medium; HAS1, 2, 3, Hyaluronan synthase 1, 2, 3; HAS2-AS1 FL, HAS2-AS1 full-length; HAS2-AS1 L, exon 2 of HAS2-AS1 long isoform; HAS2-AS1 S, exon 2 of HAS2-AS1 short isoform; HER2, epidermal growth factor receptor 2; IL24, Interleukin 24; KEGG, Kyoto Encyclopedia of Genes and Genomes; lncRNA, long non-coding RNA; miRNA, microRNA; MTT, 3-(4,5-dimethylthiazol-2-yl)-2,5-diphenyltetrazo-lium bromide; NCKAP1L, NCK associated protein 1 like; PR, progesterone receptor; RHAMM, Receptor for HA-mediated motility; RPMI 1640, Roswell Park Memorial Institute 1640 medium; SEM, Standard error of the mean; TENM1, Teneurin Transmembrane Protein 1; TFF1, Trefoil Factor 1; TGF-beta, Transforming growth factor-beta; TNBC, triple-negative breast cancer

[1]These authors contributed equally to this work.

References

[1] H. Sung, J. Ferlay, R.L. Siegel, M. Laversanne, I. Soerjomataram, A. Jemal, F. Bray, Global cancer statistics 2020: GLOBOCAN estimates of incidence and mortality worldwide for 36 cancers in 185 countries, CA Cancer J. Clin. 71 (2021), doi: 10.3322/caac.21660.

[2] T.C. Putti, D.M.A. El-Rehim, E.A. Rakha, C.E. Paish, A.H. Lee, S.E. Pinder, I.O. Ellis, Estrogen receptor-negative breast carcinomas: a review of morphology and immunophenotypical analysis, Mod. Pathol. 18 (2004) 26–35 2005 18:1, doi: 10.1038/modpathol.3800255.

[3] I.E. Smith, M. Dowsett, Aromatase inhibitors in breast cancer, N. Engl. J. Med. 348 (2003) 2431–2442, doi: 10.1056/NEJMra023246.

[4] H. Dillekås, M.S. Rogers, O. Straume, Are 90% of deaths from cancer caused by metastases? Cancer Med. 8 (2019) 5574–5576, doi: 10.1002/cam4.2474.

[5] D. Hanahan, R.A. Weinberg, Hallmarks of cancer: the next generation, Cell 144 (2011) 646–674, doi: 10.1016/j.cell.2011.02.013.

[6] I. Caon, B. Bartolini, A. Parnigoni, E. Caravà, P. Moretto, M. Viola, E. Karousou, D. Vigetti, A. Passi, Revisiting the hallmarks of cancer: the role of hyaluronan, Semin. Cancer Biol. 62 (2020) 9–19, doi: 10.1016/j.semcancer.2019.07.007.

[7] N.K. Karamanos, Z. Piperigkou, A.D. Theocharis, H. Watanabe, M. Franchi, S. Baud, S. Brézillon, M. Götte, A. Passi, D. Vigetti, S. Ricard-Blum, R.D. Sanderson, T. Neill, R.v. Iozzo, Proteoglycan chemical diversity drives multifunctional cell regulation and therapeutics, Chem. Rev. 118 (2018) 9152–9232, doi: 10.1021/acs.chemrev.8b00354.

[8] D. Manou, I. Caon, P. Bouris, I.E. Triantaphyllidou, C. Giaroni, A. Passi, N.K. Karamanos, D. Vigetti, A.D. Theocharis, The complex interplay between extracellular matrix and cells in tissues, Methods Mol. Biol. 1952 (2019) 1–20, doi: 10.1007/978-1-4939-9133-4_1.

[9] I. Caon, A. Parnigoni, M. Viola, E. Karousou, A. Passi, D. Vigetti, Cell energy metabolism and hyaluronan synthesis, J. Histochem. Cytochem. (2020), doi: 10.1369/0022155420929772.

[10] D. Vigetti, E. Karousou, M. Viola, S. Deleonibus, G. de Luca, A. Passi, Hyaluronan: biosynthesis and signaling, Biochim. Biophys. Acta Gener. Subj. 1840 (2014) 2452–2459, doi: 10.1016/j.bbagen.2014.02.001.

[11] P. Auvinen, R. Tammi, J. Parkkinen, M. Tammi, U. Ågren, R. Johansson, P. Hirvikoski, M. Eskelinen, V.M. Kosma, Hyaluronan in peritumoral stroma and malignant cells associates with breast cancer spreading and predicts survival, Am. J. Pathol. 156 (2000) 529–536, doi: 10.1016/S0002-9440(10)64757-8.

[12] P. Heldin, C.Y. Lin, C. Kolliopoulos, Y.H. Chen, S.S. Skandalis, Regulation of hyaluronan biosynthesis and clinical impact of excessive hyaluronan production, Matrix Biol. 78–79 (2019) 100–117, doi: 10.1016/j.matbio.2018.01.017.

[13] R.H. Tammi, A. Kultti, V.M. Kosma, R. Pirinen, P. Auvinen, M.I. Tammi, Hyaluronan in human tumors: pathobiological and prognostic messages from cell-associated and stromal hyaluronan, Semin. Cancer Biol. 18 (2008) 288–295, doi: 10.1016/j.semcancer.2008.03.005.

[14] D.L. Vitale, I. Caon, A. Parnigoni, I. Sevic, F.M. Spinelli, A. Icardi, A. Passi, D. Vigetti, L. Alaniz, Initial identification of UDP-glucose dehydrogenase as a prognostic marker in breast cancer patients, which facilitates epirubicin resistance and regulates hyaluronan synthesis in MDA-MB-231 cells, Biomolecules 11 (2021) 1–31, doi: 10.3390/biom11020246.

[15] R.K. Sironen, M. Tammi, R. Tammi, P.K. Auvinen, M. Anttila, V.M. Kosma, Hyaluronan in human malignancies, Exp. Cell. Res. 317 (2011) 383–391, doi: 10.1016/j.yexcr.2010.11.017.

[16] A. Passi, D. Vigetti, Hyaluronan as tunable drug delivery system, Adv. Drug. Deliv. Rev. 146 (2019) 83–96, doi: 10.1016/j.addr.2019.08.006.

[17] E. Karousou, S. Misra, S. Ghatak, K. Dobra, M. Götte, D. Vigetti, A. Passi, N.K. Karamanos, S.S. Skandalis, Roles and targeting of the HAS/hyaluronan/CD44 molecular system in cancer, Matrix Biol. 59 (2017) 3–22, doi: 10.1016/j.matbio.2016.10.001.

[18] A. Passi, D. Vigetti, S. Buraschi, R.v. Iozzo, Dissecting the role of hyaluronan synthases in the tumor microenvironment, FEBS J. 286 (2019) 2937–2949, doi: 10.1111/febs.14847.

[19] P. Heldin, K. Basu, I. Kozlova, H. Porsch, HAS2 and CD44 in breast tumorigenesis, Advances in Cancer Research, Academic Press Inc., 2014, pp. 211–229, doi: 10.1016/B978-0-12-800092-2.00008-3.

[20] M. Vanneste, V. Hanoux, M. Bouakka, P.J. Bonnamy, Hyaluronate synthase-2 overexpression alters estrogen dependence and induces histone deacetylase inhibitor-like effects on ER-driven genes in MCF7 breast tumor cells, Mol. Cell. Endocrinol. 444 (2017) 48–58, doi: 10.1016/j.mce.2017.01.046.

[21] V. Hanoux, J. Eguida, E. Fleurot, J. Levallet, P.J. Bonnamy, Increase in hyaluronic acid degradation decreases the expression of estrogen receptor alpha in MCF7 breast cancer cell line, Mol. Cell. Endocrinol. 476 (2018) 185–197, doi: 10.1016/j.mce.2018.05.008.

[22] N. Itano, L. Zhuo, K. Kimata, Impact of the hyaluronan-rich tumor microenvironment on cancer initiation and progression, Cancer Sci. 99 (2008) 1720–1725, doi: 10.1111/j.1349-7006.2008.00885.x.

[23] B. Bernert, H. Porsch, P. Heldin, Hyaluronan synthase 2 (HAS2) promotes breast cancer cell invasion by suppression of tissue metalloproteinase inhibitor 1 (TIMP-1), J. Biol. Chem. 286 (2011) 42349–42359, doi: 10.1074/jbc.M111.278598.

[24] H. Okuda, A. Kobayashi, B. Xia, M. Watabe, S.K. Pai, S. Hirota, F. Xing, W. Liu, P.R. Pandey, K. Fukuda, V. Modur, A. Ghosh, A. Wilber, K. Watabe, Hyaluronan synthase HAS2 promotes tumor progression in bone by stimulating the interaction of breast cancer stem-like cells with macrophages and stromal cells, Cancer Res. 72 (2012) 537–547, doi: 10.1158/0008-5472.CAN-11-1678.

[25] M. Wu, M. Cao, Y. He, Y. Liu, C. Yang, Y. Du, W. Wang, F. Gao, A novel role of low molecular weight hyaluronan in breast cancer metastasis, FASEB J. 29 (2015) 1290–1298, doi: 10.1096/fj.14-259978.

[26] W.J. Sullivan, P.J. Mullen, E.W. Schmid, A. Flores, M. Momcilovic, M.S. Sharpley, D. Jelinek, A.E. Whiteley, M.B. Maxwell, B.R. Wilde, U. Banerjee, H.A. Coller, D.B. Shackelford, D. Braas, D.E. Ayer, T.Q. de Aguiar Vallim, W.E. Lowry, H.R. Christofk, Extracellular matrix remodeling regulates glucose metabolism through TXNIP destabilization, Cell 175 (2018) 117–132 . e21, doi: 10.1016/j.cell.2018.08.017.

[27] S. Oikari, T. Kettunen, S. Tiainen, J. Häyrinen, A. Masarwah, M. Sudah, A. Sutela, R. Vanninen, M. Tammi, P. Auvinen, UDP-sugar accumulation drives hyaluronan synthesis in breast cancer, Matrix Biol. 67 (2018) 63–74, doi: 10.1016/j.matbio.2017.12.015.

[28] A. Barkovskaya, K. Seip, B. Hilmarsdottir, G.M. Maelandsmo, S.A. Moestue, H.M. Itkonen, O-GlcNAc transferase inhibition differentially affects breast cancer subtypes, Sci. Rep. 9 (2019), doi: 10.1038/s41598-019-42153-6.

[29] D. Vigetti, S. Deleonibus, P. Moretto, E. Karousou, M. Viola, B. Bartolini, V.C. Hascall, M. Tammi, G. de Luca, A. Passi, Role of UDP-N-acetylglucosamine (GlcNAc) and O-GlcNacylation of hyaluronan synthase 2 in the control of chondroitin sulfate and hyaluronan synthesis, J. Biol. Chem. 287 (2012) 35544–35555, doi: 10.1074/jbc.M112.402347.

[30] C.J. Narvaez, D. Grebenc, S. Balinth, J.E. Welsh, Vitamin D regulation of HAS2, hyaluronan synthesis and metabolism in triple negative breast cancer cells, J. Steroid Biochem. Mol. Biol. 201 (2020), doi: 10.1016/j.jsbmb.2020.105688.

[31] T.T. Karalis, A. Chatzopoulos, A. Kondyli, A.J. Aletras, N.K. Karamanos, P. Heldin, S.S. Skandalis, Salicylate suppresses the oncogenic hyaluronan network in metastatic breast cancer cells, Matrix Biol. Plus (2020) 6–7, doi: 10.1016/j.mbplus.2020.100031.

[32] I. Caon, M.L. D'angelo, B. Bartolini, E. Caravà, A. Parnigoni, F. Contino, P. Cancemi, P. Moretto, N.K. Karamanos, A. Passi, D. Vigetti, E. Karousou, M. Viola, The secreted protein c10orf118 is a new regulator of hyaluronan synthesis involved in tumour-stroma cross-talk, Cancers 13 (2021) 1–22, doi: 10.3390/cancers13051105.

[33] T.T. Karalis, P. Heldin, D.H. Vynios, T. Neill, S. Buraschi, R.v. Iozzo, N.K. Karamanos, S.S. Skandalis, Tumor-suppressive functions of 4-MU on breast cancer cells of different ER status: Regulation of hyaluronan/HAS2/CD44 and specific matrix effectors, Matrix Biol. 78–79 (2019) 118–138, doi: 10.1016/j.matbio.2018.04.007.

[34] H. Urakawa, Y. Nishida, J. Wasa, E. Arai, L. Zhuo, K. Kimata, E. Kozawa, N. Futamura, N. Ishiguro, Inhibition of hyaluronan synthesis in breast cancer cells by 4-methylumbelliferone suppresses tumorigenicity *in vitro* and metastatic lesions of bone *in vivo*, Int. J. Cancer 130 (2012) 454–466, doi: 10.1002/ijc.26014.

[35] Y. Li, L. Li, T.J. Brown, P. Heldin, Silencing of hyaluronan synthase 2 suppresses the malignant phenotype of invasive breast cancer cells, Int. J. Cancer 120 (2007) 2557–2567, doi: 10.1002/ijc.22550.

[36] I. Kakizaki, K. Kojima, K. Takagaki, M. Endo, R. Kannagi, M. Ito, Y. Maruo, H. Sato, T. Yasuda, S. Mita, K. Kimata, N. Itano, A novel mechanism for the inhibition of hyaluronan

biosynthesis by 4-methylumbelliferone, J. Biol. Chem. 279 (2004) 33281–33289, doi: 10.1074/jbc.M405918200.
[37] N. Nagy, T. Freudenberger, A. Melchior-Becker, K. Röck, M. ter Braak, H. Jastrow, M. Kinzig, S. Lucke, T. Suvorava, G. Kojda, A.A. Weber, F. Sörgel, B. Levkau, S. Ergün, J.W. Fischer, Inhibition of hyaluronan synthesis accelerates murine atherosclerosis: novel insights into the role of hyaluronan synthesis, Circulation 122 (2010) 2313–2322, doi: 10.1161/CIRCULATIONAHA.110.972653.
[38] D. Vigetti, M. Viola, E. Karousou, S. Deleonibus, K. Karamanou, G. de Luca, A. Passi, Epigenetics in extracellular matrix remodeling and hyaluronan metabolism, FEBS J. 281 (2014) 4980–4992, doi: 10.1111/febs.12938.
[39] S.J. Andrews, J.A. Rothnagel, Emerging evidence for functional peptides encoded by short open reading frames, Nat. Rev. Genet. 15 (2014) 193–204, doi: 10.1038/nrg3520.
[40] M. Ye, J. Zhang, M. Wei, B. Liu, K. Dong, Emerging role of long noncoding RNA-encoded micropeptides in cancer, Cancer Cell Int. 20 (2020), doi: 10.1186/s12935-020-01589-x.
[41] A. Parnigoni, I. Caon, P. Moretto, M. Viola, E. Karousou, A. Passi, D. Vigetti, The role of the multifaceted long noncoding RNAs: a nuclear-cytosolic interplay to regulate hyaluronan metabolism, Matrix Biol. Plus (2021) 100060, doi: 10.1016/j.mbplus.2021.100060.
[42] D. Vigetti, S. Deleonibus, P. Moretto, T. Bowen, J.W. Fischer, M. Grandoch, A. Oberhuber, D.C. Love, J.A. Hanover, R. Cinquetti, E. Karousou, M. Viola, M.L. D'Angelo, V.C. Hascall, G. de Luca, A. Passi, Natural antisense transcript for hyaluronan synthase 2 (HAS2-AS1) induces transcription of HAS2 via protein O-GlcNAcylation, J. Biol. Chem. 289 (2014) 28816–28826, doi: 10.1074/jbc.M114.597401.
[43] D.R. Michael, A.O. Phillips, A. Krupa, J. Martin, J.E. Redman, A. Altaher, R.D. Neville, J. Webber, M.Y. Kim, T. Bowen, The human hyaluronan synthase 2 (HAS2) gene and its natural antisense RNA exhibit coordinated expression in the renal proximal tubular epithelial cell, J. Biol. Chem. 286 (2011) 19523–19532, doi: 10.1074/jbc.M111.233916.
[44] H. Chao, A.P. Spicer, Natural antisense mRNAs to hyaluronan synthase 2 inhibit hyaluronan biosynthesis and cell proliferation, J. Biol. Chem. 280 (2005) 27513–27522, doi: 10.1074/jbc.M411544200.
[45] G. Zhu, S. Wang, J. Chen, Z. Wang, X. Liang, X. Wang, J. Jiang, J. Lang, L. Li, Long noncoding RNA HAS2-AS1 mediates hypoxia-induced invasiveness of oral squamous cell carcinoma, Mol. Carcinog. 56 (2017) 2210–2222, doi: 10.1002/mc.22674.
[46] L. Zhang, H. Wang, M. Xu, F. Chen, W. Li, H. Hu, Q. Yuan, Y. Su, X. Liu, J. Wuri, T. Yan, Long noncoding RNA HAS2-AS1 promotes tumor progression in glioblastoma via functioning as a competing endogenous RNA, J. Cell. Biochem. 121 (2020) 661–671, doi: 10.1002/jcb.29313.
[47] J. Wang, Y. Zhang, A. You, J. Li, J. Gu, G. Rao, X. Ge, K. Zhang, H. Fu, X. Liu, J. Li, Q. Wang, X. Wu, L. Cheng, M. Zhu, D. Wang, HAS2-AS1 acts as a molecular sponge for miR-137 and promotes the invasion and migration of glioma cells by targeting EZH2, Cell Cycle (2020), doi: 10.1080/15384101.2020.1826237.
[48] J. Wang, J. Gu, A. You, J. Li, Y. Zhang, G. Rao, X. Ge, K. Zhang, J. Li, X. Liu, Q. Wang, T. Lin, L. Cheng, M. Zhu, X. Wu, D. Wang, The transcription factor USF1 promotes glioma cell invasion and migration by activating lncRNA HAS2-AS1, Biosci. Rep. 40 (2020), doi: 10.1042/BSR20200487.
[49] L. Tong, Y. Wang, Y. Ao, X. Sun, CREB1 induced lncRNA HAS2-AS1 promotes epithelial ovarian cancer proliferation and invasion via the miR-466/RUNX2 axis, Biomed. Pharmacother. 115 (2019) 108891, doi: 10.1016/j.biopha.2019.108891.
[50] P. Sun, L. Sun, J. Cui, L. Liu, Q. He, Long noncoding RNA HAS2-AS1 accelerates non-small cell lung cancer chemotherapy resistance by targeting LSD1/EphB3 pathway, Am. J. Transl. Res. 12 (2020) 950–958 http://www.ncbi.nlm.nih.gov/pubmed/32269726 (accessed December 2, 2020).
[51] C. Kolliopoulos, C.Y. Lin, C.H. Heldin, A. Moustakas, P. Heldin, Has2 natural antisense RNA and Hmga2 promote Has2 expression during TGFβ-induced EMT in breast cancer, Matrix Biol. 80 (2019) 29–45, doi: 10.1016/j.matbio.2018.09.002.
[52] M. Ghandi, F.W. Huang, J. Jané-Valbuena, G. v. Kryukov, C.C. Lo, E.R. McDonald, J. Barretina, E.T. Gelfand, C.M. Bielski, H. Li, K. Hu, A.Y. Andreev-Drakhlin, J. Kim, J.M. Hess, B.J. Haas, F. Aguet, B.A. Weir, M. v. Rothberg, B.R. Paolella, M.S. Lawrence, R. Akbani, Y. Lu, H.L. Tiv, P.C. Gokhale, A. de Weck, A.A. Mansour, C. Oh, J. Shih, K. Hadi, Y. Rosen, J. Bistline, K. Venkatesan, A. Reddy, D. Sonkin, M. Liu, J. Lehar, J.M. Korn, D.A. Porter, M.D. Jones, J. Golji, G. Caponigro, J.E. Taylor, C.M. Dunning, A.L. Creech, A.C. Warren, J.M. McFarland, M. Zamanighomi, A. Kauffmann, N. Stransky, M. Imielinski, Y.E. Maruvka, A.D. Cherniack, A. Tsherniak, F. Vazquez, J.D. Jaffe, A.A. Lane, D.M. Weinstock, C.M. Johannessen, M.P. Morrissey, F. Stegmeier, R. Schlegel, W.C. Hahn, G. Getz, G.B. Mills, J.S. Boehm, T.R. Golub, L.A. Garraway, W.R. Sellers, Next-generation characterization of the Cancer Cell Line Encyclopedia, Nature 569 (2019) 503, doi: 10.1038/S41586-019-1186-3.
[53] M. Liu, C. Tolg, E. Turley, Dissecting the dual nature of hyaluronan in the tumor microenvironment, Front. Immunol. 10 (2019) 947, doi: 10.3389/fimmu.2019.00947.
[54] Y. Yung, L. Ophir, G.M. Yerushalmi, M. Baum, A. Hourvitz, E. Maman, HAS2-AS1 is a novel LH/hCG target gene regulating HAS2 expression and enhancing cumulus cells migration, J. Ovarian Res. 12 (2019) 21, doi: 10.1186/s13048-019-0495-3.
[55] X. Yang, F. Qi, S. Wei, L. Lin, X. Liu, The transcription factor C/EBPβ promotes HFL-1 cell migration, proliferation, and inflammation by activating lncRNA HAS2-AS1 in hypoxia, Front. Cell Dev. Biol. 9 (2021) 651913, doi: 10.3389/FCELL.2021.651913.
[56] I. Caon, B. Bartolini, P. Moretto, A. Parnigoni, E. Caravà, D.L. Vitale, L. Alaniz, M. Viola, E. Karousou, G. de Luca, V.C. Hascall, A. Passi, D. Vigetti, Sirtuin 1 reduces hyaluronan synthase 2 expression by inhibiting nuclear translocation of NF-κB and expression of the long-noncoding RNA HAS2−AS1, J. Biol. Chem. 295 (2020) 3485–3496, doi: 10.1074/jbc.RA119.011982.
[57] J.B. Pierce, M.W. Feinberg, Long noncoding RNAs in atherosclerosis and vascular injury, Arterioscler. Thromb. Vascular Biol. 40 (2020) 2002–2017, doi: 10.1161/ATVBAHA.120.314222.
[58] M.D. Ballantyne, K. Pinel, R. Dakin, A.T. Vesey, L. Diver, R. Mackenzie, R. Garcia, P. Welsh, N. Sattar, G. Hamilton, N. Joshi, M.R. Dweck, J.M. Miano, M.W. McBride, D.E. Newby, R.A. McDonald, A.H. Baker, Smooth muscle enriched long noncoding RNA (SMILR) regulates cell proliferation, Circulation 133 (2016) 2050, doi: 10.1161/CIRCULATIONAHA.115.021019.

[59] Y. Lu, G. Guo, R. Hong, X. Chen, Y. Sun, F. Liu, Z. Zhang, X. Jin, J. Dong, K. Yu, X. Yang, Y. Nan, Q. Huang, LncRNA HAS2-AS1 promotes glioblastoma proliferation by sponging miR-137, Front. Oncol. 11 (2021) 634893, doi: 10.3389/FONC.2021.634893.

[60] Z. Zhao, T. Liang, S. Feng, Silencing of HAS2-AS1 mediates PI3K/AKT signaling pathway to inhibit cell proliferation, migration, and invasion in glioma, J. Cell. Biochem. 120 (2019) 11510–11516, doi: 10.1002/JCB.28430.

[61] P. Heldin, K. Basu, I. Kozlova, H. Porsch, HAS2 and CD44 in breast tumorigenesis, Adv. Cancer. Res. 123 (2014) 211–229, doi: 10.1016/B978-0-12-800092-2.00008-3.

[62] Y. Lu, G. Guo, R. Hong, X. Chen, Y. Sun, F. Liu, Z. Zhang, X. Jin, J. Dong, K. Yu, X. Yang, Y. Nan, Q. Huang, LncRNA HAS2-AS1 promotes glioblastoma proliferation by sponging miR-137, Front. Oncol. 11 (2021) 634893, doi: 10.3389/FONC.2021.634893.

[63] Z. Wang, H.H. Sha, H.J. Li, Functions and mechanisms of miR-186 in human cancer, Biomed. Pharmacother. 119 (2019) 109428, doi: 10.1016/J.BIOPHA.2019.109428.

[64] K. Yao, L. He, Y. Gan, Q. Zeng, Y. Dai, J. Tan, MiR-186 suppresses the growth and metastasis of bladder cancer by targeting NSBP1, Diagn. Pathol. (2015) 10, doi: 10.1186/S13000-015-0372-3.

[65] J. Lu, Z. Zhao, Y. Ma, miR-186 represses proliferation, migration, invasion, and EMT of hepatocellular carcinoma via directly targeting CDK6, Oncol. Res. 28 (2020) 509, doi: 10.3727/096504020X15954139263808.

[66] H. Hugo, M.L. Ackland, T. Blick, M.G. Lawrence, J.A. Clements, E.D. Williams, E.W. Thompson, Epithelial−mesenchymal and mesenchymal−epithelial transitions in carcinoma progression, J. Cell. Physiol. 213 (2007) 374–383, doi: 10.1002/JCP.21223.

[67] C.M. Nelson, D. Khauv, M.J. Bissell, D.C. Radisky, Change in cell shape is required for matrix metalloproteinase-induced epithelial-mesenchymal transition of mammary epithelial cells, J. Cell. Biochem. 105 (2008) 25, doi: 10.1002/JCB.21821.

[68] J.B. Wyckoff, J.E. Segall, J.S. Condeelis, The collection of the motile population of cells from a living tumor, Cancer Res. 60 (2000).

[69] R.M. Melero-Fernandez de Mera, U.T. Arasu, R. Kärnä, S. Oikari, K. Rilla, D. Vigetti, A. Passi, P. Heldin, M.I. Tammi, A.J. Deen, Effects of mutations in the post-translational modification sites on the trafficking of hyaluronan synthase 2 (HAS2), Matrix Biol. 80 (2019) 85–103, doi: 10.1016/j.matbio.2018.10.004.

[70] R.H. Tammi, A.G. Passi, K. Rilla, E. Karousou, D. Vigetti, K. Makkonen, M.I. Tammi, Transcriptional and post-translational regulation of hyaluronan synthesis, FEBS J. 278 (2011) 1419–1428, doi: 10.1111/j.1742-4658.2011.08070.x.

[71] S. Misra, P. Heldin, V.C. Hascall, N.K. Karamanos, S.S. Skandalis, R.R. Markwald, S. Ghatak, HA/CD44 interactions as potential targets for cancer therapy, FEBS J. 278 (2011) 1429, doi: 10.1111/J.1742-4658.2011.08071.X.

[72] K. Saavalainen, S. Pasonen-Seppänen, T.W. Dunlop, R. Tammi, M.I. Tammi, C. Carlberg, The human hyaluronan synthase 2 gene is a primary retinoic acid and epidermal growth factor responding gene, J. Biol. Chem. 280 (2005) 14636–14644, doi: 10.1074/JBC.M500206200.

[73] Y. Yamaguchi, H. Yamamoto, Y. Tobisawa, F. Irie, TMEM2: A missing link in hyaluronan catabolism identified? Matrix Biol. 78−79 (2019) 139–146, doi: 10.1016/J.MATBIO.2018.03.020.

[74] M. He, Q. Jin, C. Chen, Y. Liu, X. Ye, Y. Jiang, F. Ji, H. Qian, D. Gan, S. Yue, W. Zhu, T. Chen, The miR-186-3p/EREG axis orchestrates tamoxifen resistance and aerobic glycolysis in breast cancer cells, Oncogene 38 (2019) 5551–5565 2019 38:28, doi: 10.1038/s41388-019-0817-3.

[75] M. Farooqui, L.R. Bohrer, N.J. Brady, P. Chuntova, S.E. Kemp, C.T. Wardwell, A.C. Nelson, K.L. Schwertfeger, Epiregulin contributes to breast tumorigenesis through regulating matrix metalloproteinase 1 and promoting cell survival, Mol. Cancer 14 (2015), doi: 10.1186/S12943-015-0408-Z.

[76] S.J. Prest, F.E.B. May, B.R. Westley, The estrogen-regulated protein, TFF1, stimulates migration of human breast cancer cells, FASEB J. 16 (2002) 592–594, doi: 10.1096/FJ.01-0498FJE.

[77] Y. Teng, H. Qin, A. Bahassan, N.G. Bendzunas, E.J. Kennedy, J. Cowell, The WASF3-NCKAP1-CYFIP1 complex is essential for breast cancer metastasis, Cancer Res. 76 (2016) 5133, doi: 10.1158/0008-5472.CAN-16-0562.

[78] Y. Bai, Y. Zhan, B. Yu, W.W. Wang, L. Wang, J. Zhou, R. Chen, F. Zhang, X. Zhao, W. Duan, Y. Wang, J. Liu, J. Bao, Z.Y. Zhang, X. Liu, A novel tumor-suppressor, CDH18, inhibits glioma cell invasiveness Via UQCRC2 and correlates with the prognosis of glioma patients, Cell. Physiol. Biochem. 48 (2018) 1755–1770, doi: 10.1159/000492317.

[79] W. Zhu, L. Wei, H. Zhang, J. Chen, X. Qin, Oncolytic adenovirus armed with IL-24 inhibits the growth of breast cancer *in vitro* and *in vivo*, J. Exp. Clin. Cancer Res. CR 31 (2012) 51, doi: 10.1186/1756-9966-31-51.

[80] M. Zheng, D. Bocangel, B. Doneske, A. Mhashilkar, R. Ramesh, K.K. Hunt, S. Ekmekcioglu, R.B. Sutton, N. Poindexter, E.A. Grimm, S. Chada, Human interleukin 24 (MDA-7/IL-24) protein kills breast cancer cells via the IL-20 receptor and is antagonized by IL-10, Cancer Immunol. Immunother. 56 (2006) 205–215 2006 56:2, doi: 10.1007/S00262-006-0175-1.

[81] C. Yang, Y. Tong, W. Ni, J. Liu, W. Xu, L. Li, X. Liu, H. Meng, W. Qian, Inhibition of autophagy induced by overexpression of mda-7/interleukin-24 strongly augments the antileukemia activity *in vitro* and *in vivo*, Cancer Gene Ther. 17 (2009) 109–119 2010 17:2, doi: 10.1038/cgt.2009.57.

[82] A. Sanyal, B.R. Lajoie, G. Jain, J. Dekker, The long-range interaction landscape of gene promoters, Nature 489 (2012) 109–113 2012 489:7414, doi: 10.1038/nature11279.

[83] B. Pang, Q. Wang, S. Ning, J. Wu, X. Zhang, Y. Chen, S. Xu, Landscape of tumor suppressor long noncoding RNAs in breast cancer, J. Exp. Clin. Cancer Res. CR 38 (2019), doi: 10.1186/S13046-019-1096-0.

[84] T. Gebäck, M.M.P. Schulz, P. Koumoutsakos, M. Detmar, TScratch: a novel and simple software tool for automated analysis of monolayer wound healing assays, 10.2144/000113083. 46 (2018) 265−274. https://***doi.org/10.2144/000113083.

[85] C.A. Schneider, W.S. Rasband, K.W. Eliceiri, NIH Image to ImageJ: 25 years of image analysis, Nat. Methods 9 (2012) 671–675 2012 9:7, doi: 10.1038/nmeth.2089.

[86] D.L. Vitale, F.M. Spinelli, L. Alaniz, Determination of cell-surface hyaluronan through flow cytometry, Methods Mol. Biol. 1952 (2019) 111–116, doi: 10.1007/978-1-4939-9133-4_10.